IIETA International Information and Engineering Technology Association
Advancing the World of Information and Engineering

Journal Européen des Systèmes Automatisés
Vol. 58, No. 12, December, 2025, pp. 2525-2544
Journal homepage: http://iieta.org/journals/jesa

Performance Assessment of Static and Adaptive Maintenance Strategies Under Stochastic Conditions with Penalty-Augmented Objectives Using a Monte Carlo Simulation Approach to Reliability and Cost Optimization

Khamiss Cheikh[1*], EL Mostapha Boudi[1], Rabi Rabi[2], Hamza Mokhliss[3]

[1] Department of Mechanical Engineering, Energetic Team, Mechanical and Industrial Systems (EMISys), Mohammadia School of Engineers, Mohammed V University, Rabat 999055, Morocco
[2] Department of Physics (LPM-ERM), Faculty of Sciences and Techniques, Sultan Moulay Sliman University, Beni-Mellal 23000, Morocco
[3] Department of Physics, Laboratory of Electronics, Instrumentation and Energetics, Faculty of Sciences, Chouaib Doukkali University, El Jadida 24000, Morocco

Corresponding Author Email: khamiss_cheikh@um5.ac.ma

https://doi.org/10.18280/jesa.581207

Received: 12 October 2025
Revised: 15 December 2025
Accepted: 23 December 2025
Available online: 31 December 2025

Keywords:
CBM, Monte Carlo simulation, adaptive maintenance strategies, RUL, Wiener-process degradation model, imperfect condition monitoring

ABSTRACT

Condition-based maintenance (CBM) has become a cornerstone for optimizing the performance, reliability, and cost-efficiency of industrial systems. Traditional CBM strategies, which rely on fixed inspection intervals and static preventive maintenance thresholds, often fail to account for the stochastic nature of degradation processes and the inherent imperfections in condition monitoring. These limitations can result in suboptimal maintenance decisions, such as excessive preventive interventions or missed failures. To address these challenges, this study presents a Monte Carlo simulation framework designed to evaluate and compare static and adaptive CBM strategies under conditions of uncertainty. The framework integrates a Wiener-process degradation model, imperfect condition monitoring, adaptive inspection scheduling based on residual useful life (RUL) estimates, and dynamically recalibrated preventive maintenance thresholds. Three maintenance strategies are examined: (i) a static policy with fixed inspection intervals and constant preventive thresholds, (ii) a semi-adaptive policy with fixed inspections and adaptive preventive thresholds, and (iii) a fully adaptive policy with both dynamic inspection intervals and adaptive preventive thresholds. The performance of these strategies is assessed using a comprehensive set of metrics, including total cost, downtime, reliability, short-horizon risk, and a penalty-augmented objective function that integrates cost, reliability, and risk exposure.

1. INTRODUCTION

In contemporary industrial systems, effective maintenance strategies are crucial for ensuring operational reliability, minimizing downtime, and optimizing cost-efficiency [1]. As industries become increasingly complex, with systems that demand high performance and safety, the ability to predict and prevent failures is paramount. Maintenance plays a pivotal role in safeguarding assets, prolonging operational lifespans, and maintaining system integrity [2]. In this context, condition-based maintenance (CBM) has emerged as a promising approach. CBM utilizes condition monitoring to assess the health of assets in real time, scheduling inspections and interventions based on the observed degradation state of the system. This methodology aims to replace traditional time-based maintenance with more efficient, data-driven strategies that respond to the actual condition of the equipment [3-6].

Despite the advantages offered by CBM, its implementation is fraught with challenges primarily arising from the stochastic nature of degradation processes and the inherent imperfections of condition monitoring [7-10]. Degradation is often driven by complex, random phenomena that cannot be captured by simple deterministic models. Additionally, condition monitoring provides imperfect, noisy data that may not fully reflect the true state of degradation. These uncertainties complicate the decision-making process, as maintenance actions must be based on incomplete and potentially inaccurate information [11]. Traditional CBM strategies, which rely on fixed inspection intervals and constant preventive maintenance thresholds, fail to account for these sources of variability, potentially leading to suboptimal performance. These static policies can either result in excessive maintenance activities or, conversely, delayed interventions that may allow failures to occur before detection [12-17].

To address these limitations, adaptive maintenance decision policies have been proposed. Adaptive strategies dynamically adjust inspection frequencies and preventive thresholds in response to observed degradation and updated system information [18-22]. By recalibrating maintenance decisions

based on real-time condition data, adaptive policies aim to more precisely align maintenance activities with the evolving risk profile of the system. These adaptive policies offer the potential for more cost-effective and reliable maintenance, particularly in environments characterized by high uncertainty. However, the comparative performance of static versus adaptive strategies under realistic operational conditions remains underexplored, particularly in terms of long-term cost, reliability, and risk mitigation [23-25].

The objective of this study is to develop a robust framework for evaluating and comparing static and adaptive CBM strategies [26-30]. The framework incorporates a Wiener process degradation model (WP), representing the stochastic evolution of system degradation, alongside imperfect condition monitoring (MM) characterized by Gaussian noise. Inspection policies (IP) are formulated as either fixed intervals (ΔT_{fix}) or adaptive intervals (ΔT_k) based on residual useful life (RUL) estimates. Preventive maintenance thresholds (PM) are either static (L_m) or adaptive ($L_{m,k}$), with the latter being recalibrated based on the observed degradation state. The performance of these strategies is evaluated using a range of metrics, including the short-horizon failure probability (p_{hit}), which quantifies the likelihood of failure before the next inspection, and the Kaplan–Meier survival estimator (KM) for reliability estimation. Economic performance is assessed through the average cost rate (C_{avg}) and the PM/CM ratio, which compares preventive to corrective maintenance efforts. Additionally, a penalty-augmented objective function (J_λ) is introduced, incorporating both cost and reliability penalties to ensure a balanced trade-off between economic efficiency and operational safety [31].

This paper contributes to the field by presenting a comprehensive simulation framework that integrates these key components: degradation modeling, inspection scheduling, preventive maintenance threshold adjustment, risk quantification, and performance evaluation. The simulation framework is used to assess three maintenance policies: (i) the static policy with fixed inspections and fixed thresholds (ΔT, M), (ii) the semi-adaptive policy with fixed inspections and adaptive thresholds (ΔT, M_k), and (iii) the fully adaptive policy incorporating both dynamic inspections and adaptive thresholds (ΔT_k, M_k). The study provides a detailed comparative analysis of these strategies, highlighting their relative advantages and trade-offs in terms of cost, downtime, reliability, and risk [32].

While classical P–F interval and predictive maintenance (PdM) strategies have been widely studied, this work focuses specifically on the relative behavior of static versus adaptive CBM policies under identical stochastic conditions. The proposed Monte Carlo framework is intentionally generic and can later be extended to include P–F or predictive triggers, enabling systematic benchmarking in future research.

The remainder of this paper is organized as follows. Section 2 outlines the methodological framework, including the mathematical formulations for degradation, inspections, and maintenance decision rules. Section 3 describes the three maintenance strategies under consideration. Section 4 details the Monte Carlo simulation architecture, while Section 5 explains the simulation configuration and input parameters. Section 6 presents the results and their analysis, followed by a discussion of the engineering implications in Section 7. Finally, Section 8 concludes the paper and outlines directions for future research.

2. METHODOLOGY

The methodological framework employed in this study integrates stochastic degradation modeling, noisy condition monitoring, adaptive inspection and maintenance policies, and penalty-augmented performance evaluation within a Monte Carlo simulation environment. This approach enables a rigorous comparison of integrated maintenance strategies under uncertainty by capturing both the stochastic dynamics of degradation and the economic and reliability consequences of maintenance actions [33, 34].

The stochastic degradation process is represented by a Wiener process with drift. Its dynamics are expressed as [35]:

$$dX(t) = \mu dt + \sigma dW(t), X(0) = X_0, \tag{1}$$

where, $X(t)$ is the degradation state at time t, μ is the drift coefficient representing the average degradation rate, σ is the diffusion coefficient capturing stochastic variability, and W(t) is a standard Wiener process. The system is assumed to start from the as-good-as-new state $X_0 = 0$, while failure is defined as the first hitting time of the critical threshold L_f. Eq. (1) captures the fundamental trade-off in degradation modeling: the deterministic wear component provides predictability, while the stochastic term introduces uncertainty that complicates maintenance planning [36, 37].

Since degradation is not directly observable with perfect accuracy, inspections provide noisy measurements. The measurement model is written as [38, 39]:

$$\tilde{X}(t) = X(t) + \varepsilon, \varepsilon \sim \mathcal{N}(0, \sigma^2_{\text{meas}}), \tag{2}$$

where, $\tilde{X}(t)$ denotes the observed degradation at time *t*, and ε represents Gaussian measurement error with variance σ^2_{meas}. This formulation reflects the imperfection of sensors and monitoring technologies, ensuring that maintenance decisions are made under uncertainty rather than idealized perfect information [40, 41].

Inspections can be scheduled periodically or adaptively. In the periodic case, inspections occur at constant intervals:

$$\Delta T_{\text{fix}} = \text{constant}, \tag{3}$$

Although simple to implement, this purely time-driven strategy does not account for the evolving condition of the system [42]. Adaptive inspection strategies, in contrast, rely on RUL estimation. The expected RUL at time t is approximated by [43]:

$$\widehat{\text{RUL}}(t) = \frac{L_f - \hat{X}(t)}{\mu} \tag{4}$$

where, $\hat{X}(t)$ is a filtered estimate of the degradation state. Eq. (4) expresses the intuitive relationship that remaining life is proportional to the distance from the current condition to the failure threshold, scaled by the average wear rate. On this basis, the next inspection interval is defined as:

$$\Delta T_k = \text{clamp}\left(\alpha_T \, \widehat{\text{RUL}}(t), \Delta T_{min}, \Delta T_{max}\right), \tag{5}$$

where, α_T is the adaptation coefficient, and the clamping function ensures that inspection intervals remain within the admissible range [ΔT_{min}, ΔT_{max}]. Eq. (5) introduces adaptivity

into inspection scheduling: inspections are performed more frequently when the estimated RUL is short and less frequently when the system is in a healthier state.

Preventive maintenance is initiated when degradation exceeds a predefined threshold. In the fixed-threshold policy, the trigger is expressed as [44]:

$$L_m = \text{constant}, L_m < L_f, \tag{6}$$

Eq. (6) reflects a traditional approach, ensuring preventive actions occur before failure but without accounting for variations in system behavior. Adaptive-threshold strategies introduce greater flexibility by updating the preventive limit according to:

$$L_{m,k} = max\left(L_{min}, L_m - \alpha_L\left(L_f - \hat{X}(t)\right)\right), \tag{7}$$

Subject to the constraint:

$$L_{m,k} \leq L_f - \delta L_{\text{safety}}, \tag{8}$$

Eqs. (7) and (8) ensure that preventive thresholds are tightened as the system approaches failure, while also guaranteeing a minimal safety margin relative to L_f. The parameter α_L controls the aggressiveness of this adaptation, L_{min} prevents the threshold from being excessively conservative, and δL_{safety} enforces a buffer that guards against unsafe recalibrations.

An essential aspect of reliability assessment is the between-inspection hitting probability, which quantifies the likelihood of failure before the next inspection. For a Wiener process with drift, this probability is given by [45]:

$$p_{\text{hit}}(h \mid a) = 1 - \left[\Phi\left(\frac{a-\mu h}{\sigma\sqrt{h}}\right) - \exp\left(\frac{2\mu a}{\sigma^2}\right)\Phi\left(\frac{-a-\mu h}{\sigma\sqrt{h}}\right)\right], \tag{9}$$

where, $a = L_f - \hat{X}(t)$ denotes the current margin to failure, h is the length of the inspection interval, and $\Phi(\cdot)$ is the cumulative distribution function of the standard normal distribution. Eq. (9) provides a direct measure of the short-term risk exposure associated with inspection decisions, and forms the basis for constraint enforcement in adaptive strategies [46].

To evaluate long-term system reliability, the Kaplan–Meier survival estimator is employed [47]:

$$\hat{S}(t) = \prod_{t_j \leq t}\left(1 - \frac{d_j}{n_j}\right), \tag{10}$$

Here, d_j is the number of failures observed at time t_j, and n_j is the number of systems still at risk just before t_j. Eq. (10) provides a non-parametric estimate of the survival function, capable of handling censored data and therefore well suited to simulation environments where many systems survive until the end of the observation horizon. Economic performance is assessed through the long-run average cost rate [30]:

$$C_{\text{avg}} = \frac{1}{T_{\text{op}}}\sum_{i=1}^{N_{\text{sim}}} C_i, \tag{11}$$

where, C_i denotes the total cost in the i-th simulation. Eq. (11) aggregates the costs of inspections, preventive interventions, and corrective repairs into a single normalized performance measure. To further characterize the balance between preventive and corrective actions, the ratio:

$$\text{PM/CM Ratio} = \frac{\mathbb{E}[N_{\text{PM}}]}{max(\mathbb{E}[N_{\text{CM}}], \varepsilon)}, \tag{12}$$

Is introduced, where $\mathbb{E}[N_{\text{PM}}]$ and $\mathbb{E}[N_{\text{CM}}]$ are the expected numbers of preventive and corrective actions, and ε is a small constant avoiding division by zero. This ratio highlights whether a strategy is more preventive-oriented or failure-driven.

Finally, to unify cost efficiency with reliability and risk requirements, a penalty-augmented objective function is defined [48]:

$$J_\lambda = C_{avg} + \lambda_R \max\left(0, R_{\min} - R_{R_{\text{time}}}\right) + \lambda_{\text{hit}}\,\mathbb{E}\left[\mathbf{1}_{\{p_{\text{hit}} > \beta\}}\right] \tag{13}$$

The first term represents the economic cost rate, the second term imposes penalties when the reliability at the reporting horizon $R_{R\text{time}}$ falls below the required minimum $R_{\min}$, and the third penalizes cases where the between-inspection failure probability exceeds the admissible tolerance β. The penalty weights λ_R and λ_{hit} emphasize the primacy of safety and reliability in industrial applications, ensuring that strategies which fail to meet these requirements cannot be regarded as competitive, regardless of their apparent cost efficiency [49, 50].

Eqs. (1) through (13) thus provide the mathematical backbone of the methodology. The degradation dynamics (Eqs. (1)-(2)), inspection rules (Eqs. (3)-(5)), preventive thresholds (Eqs. (6)-(8)), risk measures (Eq. (9)), reliability evaluation (Eq. (10)), economic indicators (Eqs. (11)-(12)), and penalty-augmented objective (Eq. (13)) establish a comprehensive and internally consistent framework for evaluating CMB ategies.

To ensure robustness, key adaptive and measurement parameters (α_T, α_L, σ_{meas}) were later varied within realistic bounds (see Section 6.3). This sensitivity analysis confirmed that while numerical values of cost and reliability shift modestly, the qualitative behavior and relative ranking of strategies remain stable.

Eq. (13) is used as an exact-penalty surrogate for the constrained problem $\min C_{avg}$ subject to $R(T_{time}) \geq R_{min}$ and $p_{hit} \leq \beta$. The penalty weights λ_R and λ_{hit} are chosen 'sufficiently large' so that violations of reliability and short-horizon risk dominate the economic term, reflecting their engineering priority. In our setting, with $C_{avg} \approx 4.5$, a typical reliability shortfall $R_{min} - R(T_{time}) \approx 0.79$ implies $\lambda_R > 4.5/0.79 \approx 5.7$ already ensures dominance of the reliability penalty. Likewise, with ≈ 64% of intervals breaching β, the risk penalty dominates for $\lambda_{hit} > 4.5/0.64 \approx 7.0$. Therefore, any $\lambda_R, \lambda_{hit} \gtrsim 10$ enforce the intended priority; specific values above these thresholds do not affect qualitative conclusions.

3. ADAPTIVE MAINTENANCE DECISION POLICIES

Adaptive maintenance decision policies constitute the operational core of the CMB work. They specify how inspection schedules and preventive maintenance thresholds

are defined, either statically or adaptively, in response to observed system degradation. The three strategies examined in this study represent progressively increasing levels of adaptivity, ranging from a purely static baseline to a fully adaptive policy [51, 52]. This section details the formulation of each strategy, its governing equations, and its conceptual implications.

3.1 Strategy I: Fixed inspections and fixed threshold (ΔT, M)

The first policy, denoted (ΔT, M), represents the static benchmark (see Figure 1). Under this regime, inspections are executed periodically at constant intervals using Eq. (3).

While preventive maintenance is initiated when the observed degradation trajectory crosses a fixed threshold as you see in Eq. (6).

Eqs. (3) and (6) define a fully deterministic policy structure, in which neither the inspection cadence nor the intervention threshold is modified in response to evolving degradation states. This approach reflects long-standing industrial practice, particularly in sectors where condition monitoring is rudimentary or where regulatory frameworks mandate fixed maintenance intervals. However, it suffers from inherent inefficiencies: inspections may be redundant during periods of low degradation intensity, while they may be too sparse during accelerated deterioration phases. Likewise, the fixed threshold L_m may trigger preventive interventions either prematurely (if degradation progresses slowly) or too late (if stochastic variability accelerates failure).

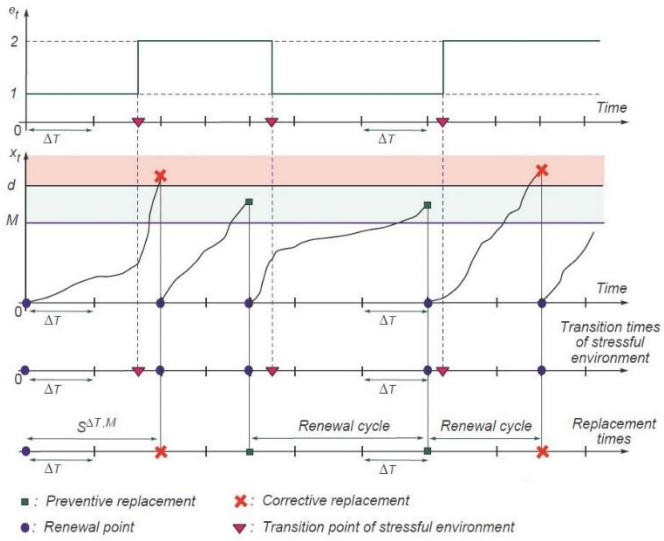

Figure 1. Principe of maintenance strategy (ΔT, M)

As such, the (ΔT, M) policy is primarily retained as a baseline reference for quantifying the incremental benefits of adaptivity.

3.2 Strategy II: Fixed inspections and adaptive threshold (ΔT, M_k)

The second policy, denoted (ΔT, M_k), preserves periodic inspections but introduces adaptivity in the preventive threshold (see Figure 2). Inspections continue to be scheduled at fixed intervals ΔT_{fix}, as in the baseline policy, but the preventive threshold is dynamically recalibrated at each inspection according to Eq. (7). Subject to the operational constraint of Eq. (8).

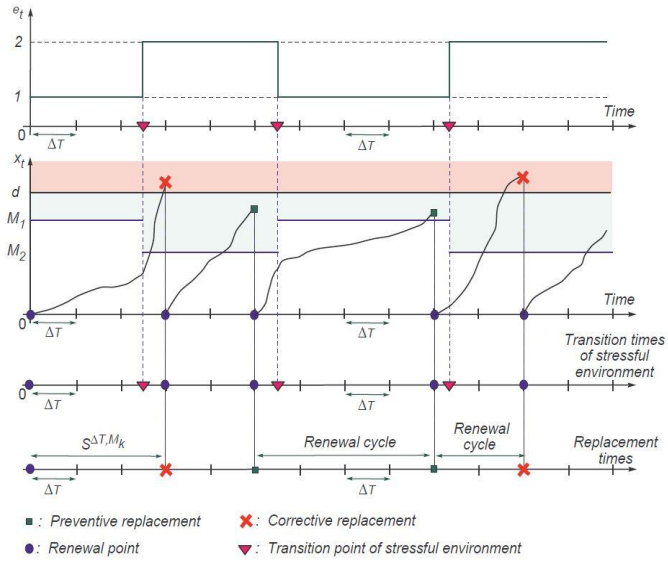

Figure 2. Principe of maintenance strategy (ΔT, M_k)

Eq. (7) introduces a linear adaptation mechanism: the preventive threshold is progressively reduced as the system approaches the failure limit L_f. The adaptation coefficient α_L regulates the aggressiveness of this recalibration, while the lower bound L_{min} prevents excessively conservative interventions. The additional constraint Eq. (8) guarantees that preventive actions always maintain a non-negligible safety buffer from failure.

Conceptually, this strategy embodies a semi-adaptive philosophy. It retains the simplicity of periodic inspections, thereby minimizing the complexity of planning, but incorporates risk sensitivity at the intervention stage. Preventive actions become more likely as degradation intensifies, which reduces the probability of unplanned corrective maintenance. However, this responsiveness may increase the frequency of preventive interventions relative to the static baseline, potentially raising cumulative costs. The (ΔT, M_k) strategy thus represents a compromise: It augments reliability by modulating preventive aggressiveness, but does not alter the inspection burden.

3.3 Strategy III: Adaptive inspections and adaptive threshold (ΔT_k, M_k)

The third strategy, denoted (ΔT_k, M_k), is the most comprehensively adaptive among those analyzed (see Figure 3). It introduces responsiveness into both inspection scheduling and preventive threshold setting. At each inspection epoch, the RUL is estimated in Eq. (4).

And the subsequent inspection interval is recalibrated dynamically using Eq. (5).

Eqs. (4)-(5) formalize a fully adaptive inspection policy: inspections accelerate as the estimated RUL shortens, thereby intensifying monitoring during high-risk phases, and relax when the system is deemed healthy. The preventive threshold is simultaneously governed by Eqs. (7)-(8), ensuring that interventions are also more conservative when failure proximity increases.

This policy represents a risk-driven paradigm in which both monitoring intensity and intervention aggressiveness evolve dynamically. By design, it minimizes exposure to undetected

failures, since inspection and intervention cadence tighten as the system approaches criticality. However, the dual adaptivity increases operational variability: Inspection workloads fluctuate, preventive interventions occur with higher frequency under rapid degradation, and planning complexity is elevated. While these characteristics may increase cost volatility, they also deliver superior reliability assurance.

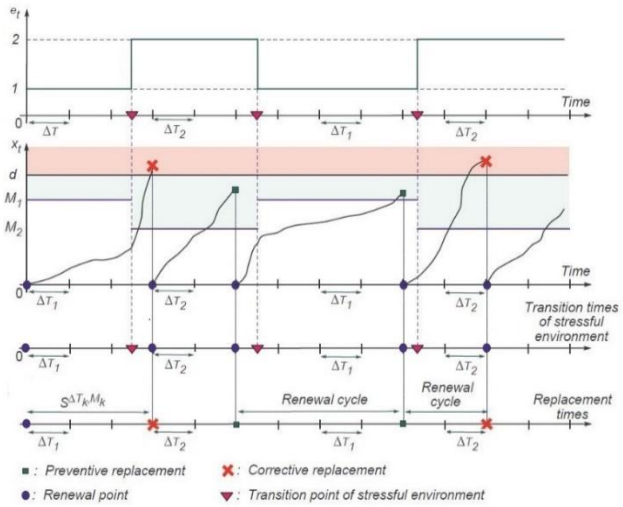

Figure 3. Principe of maintenance strategy (ΔT_k, M_k)

4. MONTE CARLO SIMULATION ARCHITECTURE

The stochastic nature of degradation processes, combined with the imperfect observability of system states, renders closed-form analytical evaluation of maintenance strategies intractable. To overcome this challenge, a Monte Carlo simulation architecture was developed, enabling the systematic replication of degradation trajectories, inspection events, maintenance decisions, and resulting cost–reliability outcomes. By generating a sufficiently large ensemble of independent realizations, the architecture provides statistically robust estimates of performance metrics and enables direct comparison of alternative strategies under identical stochastic conditions.

Each replication begins with the initialization of the system at the as-good-as-new state, X(0) = 0. The subsequent evolution of degradation is governed by the Wiener process with drift (Eq. (1)), discretized numerically using the Euler–Maruyama method. At each integration step of size Δt, the degradation state is updated according to:

$$X(t+\Delta t) = X(t) + \mu\Delta t + \sigma\sqrt{\Delta t}\xi, \xi \sim \mathcal{N}(0,1), \qquad (14)$$

This recursive formulation ensures that both the deterministic drift and the stochastic fluctuations of the degradation path are faithfully represented. The trajectory continues until the operational horizon T_{op} is reached or until a corrective failure event occurs.

Inspection epochs are determined by the strategy under evaluation. For static policies, inspections are scheduled periodically at fixed intervals as prescribed in Eq. (3). For adaptive policies, inspection times are recalibrated dynamically in accordance with RUL estimates (Eqs. (4)-(5)). At each inspection, the true degradation state is not observed directly; instead, a noisy measurement is generated via Eq. (2). This measured value is then filtered to obtain an operational estimate $\hat{X}(t)$, which serves as the basis for subsequent decision-making.

Maintenance actions are triggered according to the decision rules described in Section 3. If the observed degradation exceeds the preventive threshold (Eqs. (6) and (8)), a preventive intervention is executed, incurring cost C_{PM}, downtime t_{PM}, and resetting the degradation process to its initial state. If the degradation path reaches the failure threshold L_f before preventive action is taken, a corrective intervention is initiated. Corrective actions are substantially more disruptive, as they incur cost C_{CM} and downtime t_{CM}, reflecting both direct replacement costs and collateral losses such as production stoppages. Inspections themselves are not costless; each inspection adds C_{insp} to the total expenditure and t_{insp} to cumulative downtime, ensuring that monitoring effort is explicitly represented in the evaluation.

During each replication, several performance variables are recorded. These include the number of inspections, preventive actions, and corrective interventions, the cumulative downtime, the average cost rate (Eq. (11)), and the PM/CM ratio (Eq. (12)). In addition, the time of the first corrective maintenance is tracked to estimate the reliability function via the Kaplan–Meier estimator (Eq. (10)). Short-horizon risks are quantified at the inspection level by computing the between-inspection hitting probability using Eq. (9). Finally, the penalty-augmented performance index J_λ (Eq. (13)) is evaluated, thereby integrating cost, reliability, and risk compliance into a unified metric.

The architecture is executed over N_{sim} independent replications to ensure convergence of sample averages to their expected values. Each replication employs independent random variates, except in cases where common random numbers are applied to enhance the precision of pairwise comparisons. At the end of the simulation, ensemble averages and empirical distributions of all performance indicators are computed, enabling not only the comparison of mean outcomes but also the assessment of variability and robustness.

This Monte Carlo architecture therefore constitutes a closed-loop computational experiment: degradation trajectories evolve stochastically, inspections provide imperfect observations, decision rules determine maintenance actions, costs and downtimes are accumulated, and reliability is updated. By iterating this cycle across thousands of replications, the framework yields statistically consistent performance estimates. This architecture thus provides a rigorous basis for the comparative evaluation of static and adaptive maintenance strategies, ensuring that the reported outcomes reflect both the stochastic variability of degradation and the operational consequences of decision-making under uncertainty.

We set a priori precision goals: (i) relative 95% CI half-width for $C_{avg} \leq 1\%$ of the mean; (ii) absolute 95% CI half-widths ≤ 0.03 for the Kaplan–Meier reliability at t = 2000 and for $\Pr(p_{hit} > \beta)$. To monitor convergence, we employed replication-batch means (10 batches of 100 runs) and a half-width stopping rule.

5. SIMULATION CONFIGURATION AND INPUT PARAMETERS

The performance of the three integrated maintenance strategies ((ΔT, M), (ΔT, M_k), and (ΔT_k, M_k)) was evaluated

using a Monte Carlo simulation framework specifically designed to capture the stochastic variability of degradation processes, the imperfect nature of inspection data, and the asymmetric costs and downtimes associated with preventive and corrective interventions. The simulation was implemented with careful consideration of both statistical robustness and engineering realism, ensuring that the comparative results reflect practical operating conditions rather than theoretical simplifications.

The operational horizon was set to $T_{op} = 2 \times 10^4$ time units, which corresponds to a sufficiently long service life to observe multiple cycles of degradation and maintenance within each simulation run. This value was chosen to ensure that both preventive and corrective actions had the opportunity to occur repeatedly, thereby providing statistically meaningful estimates of costs, downtime, and reliability. To reduce stochastic noise in the results, the analysis was based on $N_{sim} = 1000$ independent replications. This sample size is large enough to stabilize Monte Carlo estimates while remaining computationally feasible. Each degradation trajectory was simulated by discretizing the governing stochastic differential equation using the Euler–Maruyama scheme with a time increment of $\Delta t = 1$. The choice of this step size reflects a compromise: it is small enough to accurately capture stochastic dynamics yet sufficiently large to avoid unnecessary computational expense. For interpretability, a subset of fifteen trajectories was retained for graphical representation, providing insight into the variability of degradation paths and maintenance outcomes across different strategies.

The underlying degradation process was modeled as a Wiener process with drift, which is widely recognized in the literature as a parsimonious yet effective representation of cumulative damage subject to random fluctuations. The governing dynamics were expressed in Eq. (1).

The drift coefficient was fixed at $\mu = 0.01$, representing a relatively slow but steady accumulation of wear or damage over time, while the diffusion parameter was set to $\sigma = 0.12$, reflecting significant environmental and operational variability that causes degradation to deviate unpredictably from its mean trajectory. The system was assumed to start from an as-good-as-new condition, $X_0 = 0$, after installation or major overhaul. Failure was defined as the first hitting time of the degradation trajectory with the critical threshold $L_f = 5$. This failure threshold can be interpreted as a physical or functional limit, such as a maximum allowable crack length, wear depth, or loss of thickness in a structural element. The chosen values generate degradation trajectories that remain within a realistic industrial range, balancing the competing influences of predictable wear and stochastic shocks. These parameter values were intentionally selected to generate a high-variance degradation environment, serving as a stress-test for the maintenance policies. The resulting low reliability levels are therefore not indicative of model failure, but rather reflect the intended difficulty of the simulation scenario, designed to expose the sensitivity and robustness of static and adaptive CBM strategies under severe stochastic variability.

Inspection processes were modeled as noisy observations of the true degradation state, consistent with practical monitoring systems where sensors and non-destructive tests introduce measurement errors. Observations at inspection times were expressed in Eq. (2), where the measurement error ε followed a Gaussian distribution with standard deviation $\sigma_{meas} = 0.05$. This value reflects the relatively high accuracy of modern condition monitoring systems, while acknowledging that no measurement system is free from noise. In the fixed inspection policy, inspections occurred at regular intervals of $\Delta T_{fix} = 120$. This interval represents a compromise between frequent monitoring, which increases costs and downtime, and sparse monitoring, which increases the risk of undetected failures. In adaptive inspection strategies, the interval between inspections was recalibrated dynamically according to estimates of RUL, such that ΔT_k is expressed using Eq. (5). The adaptation coefficient was set to $\alpha_T = 0.4$, which provides a moderate sensitivity to the estimated remaining life. To prevent unrealistic extremes, inspection intervals were bounded between $\Delta T_{max} = 360$. The minimum interval ensures that inspections cannot occur more frequently than is practically possible (e.g., due to manpower or logistical constraints), while the maximum interval guarantees that inspections are not postponed excessively, which would expose the system to unacceptable risks.

Preventive maintenance was governed by threshold-based rules. In the baseline policy, the preventive threshold was fixed at $L_m = 3.5$, a value chosen to strike a balance between premature preventive interventions, which inflate costs, and delayed interventions, which increase the risk of corrective maintenance. A lower admissible bound of $L_{min} = 2.5$ was imposed to ensure that adaptive strategies would not recalibrate thresholds to excessively conservative values, which could result in unsustainable preventive workloads. In adaptive-threshold strategies, the trigger was updated according to Eq. (7), with $\alpha_L = 0.3$. This value was selected to introduce moderate responsiveness to the proximity of failure while avoiding destabilizing oscillations in preventive policy. In addition, a mandatory safety margin was imposed such that $L_{m,k} \leq L_f - \delta L_{safety}$, with $\delta L_{safety} = 0.4$. This safety margin guarantees that preventive maintenance is always initiated at least 0.4 units below the failure threshold, thereby ensuring that no adaptation places the system at excessive risk of immediate failure.

The economic and operational impacts of interventions were explicitly quantified. Preventive maintenance was assigned a unit cost of $C_{PM} = 100$ and a downtime of $t_{PM} = 30$. These values capture the relatively modest economic and operational impact of preventive actions, which typically involve planned component replacements or adjustments. Corrective maintenance was modeled as substantially more expensive, with a unit cost of $C_{CM} = 5000$ and a downtime of $t_{CM} = 800$. This strong asymmetry reflects the realities of industrial practice, where corrective actions often require unplanned shutdowns, significant resource mobilization, and potential collateral damage. Inspections were comparatively inexpensive, with a cost of $C_{insp} = 5$ and a downtime of $t_{insp} = 5$, but their cumulative effect becomes non-negligible when inspection frequency is high. These parameters provide a realistic economic framework in which strategies must carefully balance inspection, preventive, and corrective actions.

To ensure compliance with engineering requirements, reliability and risk constraints were embedded into the evaluation. A minimum survival probability of $R_{min} = 0.95$ was imposed, with reliability estimated at a reporting horizon of $R_{time} = 2000$ using Kaplan–Meier survival analysis. This requirement reflects the expectation that in industrial settings, systems should maintain high levels of reliability over typical production cycles. In addition, a short-horizon constraint was specified, requiring that the probability of failure between consecutive inspections not exceed $\beta = 0.05$. This constraint

acknowledges that frequent risks of interim failure are unacceptable, even if long-term survival targets are nominally achieved.

Performance was therefore assessed using a penalty-augmented objective function that integrates direct costs with penalties for violations of reliability and risk requirements. The augmented cost was defined in Eq. (13), where C_{avg} represents the long-run average cost rate, R_{Rtime} is the reliability at the reporting horizon, and $1_{\{phit>\beta\}}$ is an indicator capturing whether the between-inspection risk exceeded the tolerance level. Penalty weights were fixed at $\lambda_R = 104$ and $\lambda_{hit} = 103$, reflecting the engineering principle that reliability and risk compliance are non-negotiable, and that any policy violating these requirements should be deemed unacceptable regardless of its cost efficiency.

Finally, random number control was implemented to ensure reproducibility and comparability of results. A master seed of $s_{master} = 42$ was employed for the pseudo-random number generator. When common random numbers were disabled, independent random streams were generated for each strategy by applying offsets to this seed. This approach allowed fair comparisons under synchronized stochastic conditions, while also providing realistic variability in independent replications.

We evaluated convergence using 10 replication batches of 100 runs. Batch-mean trajectories for C_{avg}, R(t = 2000), and $Pr(p_{hit} > \beta)$ showed no drift and tight overlapping CIs. Relative standard error of $\bar{C}$ was < 0.7%; absolute half-widths for R and $Pr(p_{hit} > \beta)$ were ≤ 0.03. The qualitative conclusions (constraint violations for all policies; negligible differences in means; minor tail-risk mitigation) were unchanged when re-estimating with the first 600, 800, and full 1000 replications.

These convergence diagnostics confirm that our findings are not sensitive to the number of replications and that $N_{sim} = 1000$ ensures decision-grade precision.

With observed dispersion of $\hat{\sigma}(C_{avg}) \approx 0.84–0.89$, the standard error at N = 1000 is ≤ 0.028, giving a 95% CI half-width ≤ 0.055 (< 1.3% of $\bar{C} \approx 4.5$). For reliability R ≈ 0.16, a binomial proxy yields a half-width ≈ 0.023. For $Pr(p_{hit} > \beta) \approx 0.64$, the half-width is ≈ 0.03. Thus N = 1000 satisfies our precision targets and provides conservative margin; sequential checks indicated adequacy by N ≈ 600–800. Common random numbers were applied across strategies to improve comparative efficiency.

In summary, the simulation configuration combined a Wiener-based degradation model, noisy inspection measurements, adaptive or fixed preventive thresholds, explicit cost–downtime accounting, and penalty-augmented performance evaluation within a Monte Carlo environment of 1 replication. The chosen parameter values were calibrated to reflect realistic industrial conditions, ensuring that strategies are evaluated not only on cost performance but also on their ability to satisfy stringent reliability and safety requirements. This framework thus provides a rigorous and credible experimental basis for assessing the comparative merits of integrated CBM policies.

6. RESULTS AND INTERPRETATIONS

This section presents and interprets the outcomes of the Monte Carlo simulations performed for the three integrated CBM strategies under consideration: (ΔT, M), (ΔT, M_k), and (ΔT_k, M_k). The results are organized into three parts: (i) global performance metrics, (ii) short-horizon risk and preventive trigger analysis, and (iii) penalty-augmented evaluations. Numerical evidence is provided by Tables 1-6, while complementary visual insights are conveyed through Figures 4(a)-15(c), where each subplot is denoted explicitly by a lowercase letter.

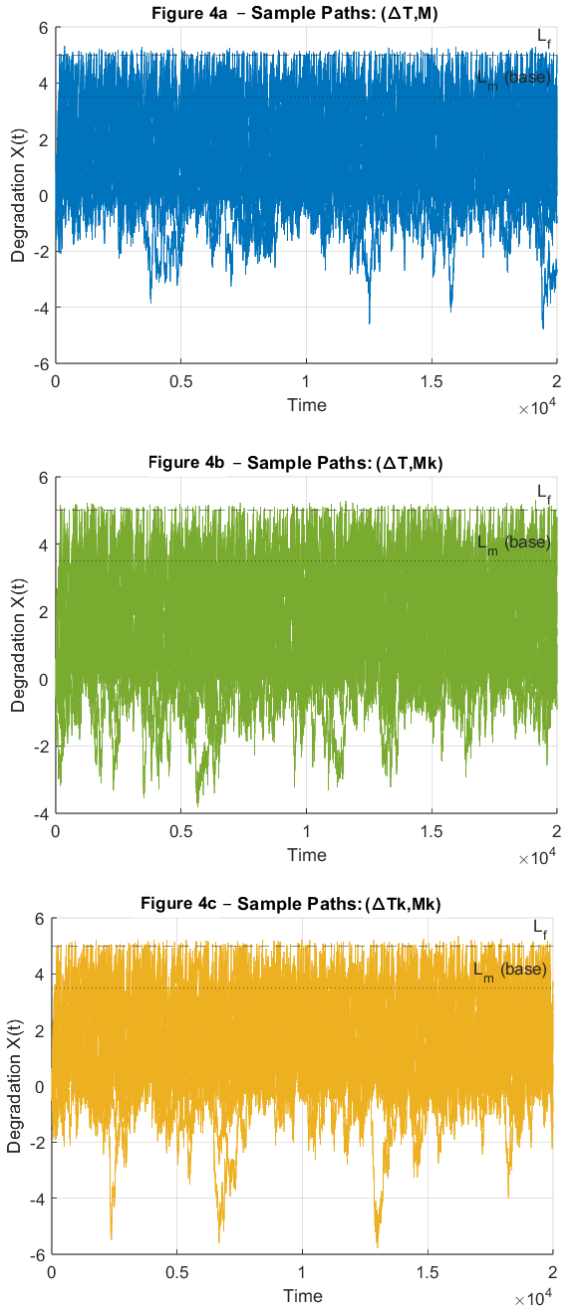

Figure 4. Sample paths for all strategies

6.1 Global cost–reliability performance

The comparative analysis of the three maintenance strategies ((ΔT, M), (ΔT, M_k), and (ΔT_k, M_k)) based on the aggregated indicators reported in Tables 1-3 and the visual evidence provided in Figures 4(a)-8(a) reveals a high degree of convergence in economic performance, inspection effort, and downtime accumulation. Despite the introduction of adaptive mechanisms in the latter two policies, the overall trajectories of costs, intervention patterns, and system reliability remain strikingly similar across strategies.

The degradation trajectories plotted in Figures 4(a)-(c)

provide a micro-level perspective on these findings. In the baseline case (Figure 4(a)), degradation paths often progress uninterrupted to the failure threshold, triggering corrective maintenance, with preventive interventions occurring sporadically. In the adaptive threshold case (Figure 4(b)), preventive interventions are sometimes initiated earlier, as the threshold adjusts downward in response to degradation estimates, yet the adjustment is insufficient to prevent many trajectories from still crossing the failure limit. In the adaptive interval case (Figure 4(c)), inspection frequency occasionally increases when degradation accelerates, but stochastic fluctuations often lead to threshold exceedances before the next inspection occurs. The qualitative similarity of the three panels illustrates why the PM/CM ratios and downtime profiles remain essentially invariant across strategies.

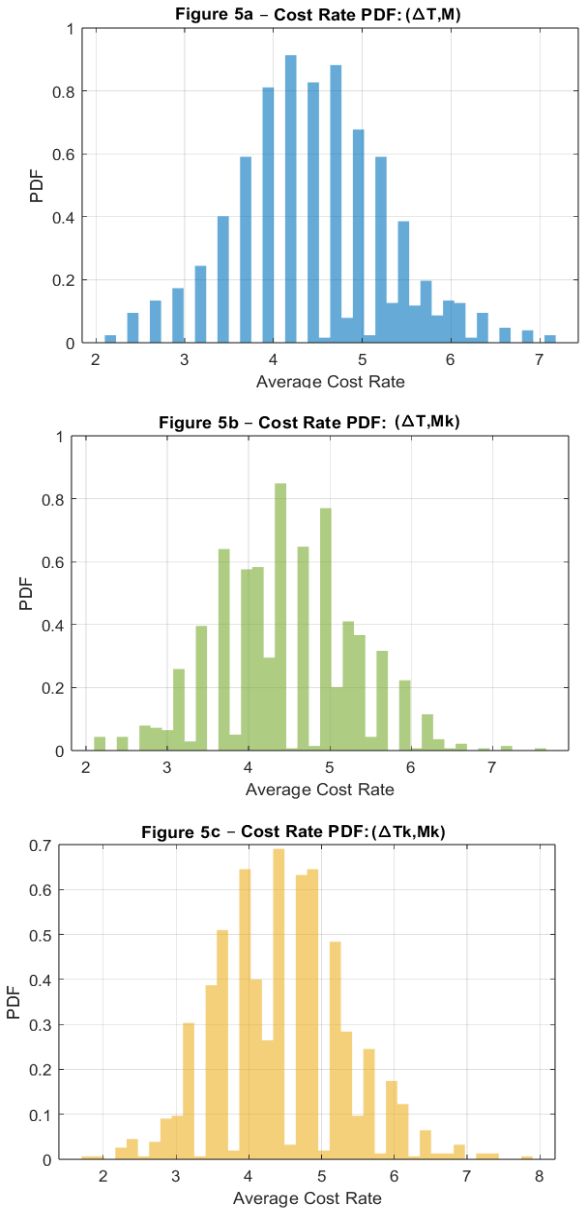

Figure 5. Cost distributions for all strategies

From an economic standpoint, the three strategies exhibit nearly indistinguishable outcomes. As shown in Table 1, the mean cost rates fall within a very narrow interval, ranging from 4.4586 for (ΔT_k, M_k) to 4.4868 for (ΔT, M). This difference of less than one percent indicates that the adoption of adaptive thresholds or intervals does not materially alter long-run cost efficiency. The stability of these results is reinforced by the moderate standard deviations (≈ 0.84–0.89), which reflect only limited dispersion due to stochastic variability. This pattern is clearly illustrated in Figures 5(a)-(c), where the cost distributions overlap almost perfectly, producing unimodal, symmetric histograms centered at virtually the same mean. A careful comparison of the three panels shows that the adaptive interval strategy (Figure 5(c)) produces a marginally thinner right tail, suggesting a slightly lower incidence of extreme cost realizations, yet the effect is far too small to be operationally significant.

The downtime statistics mirror this convergence. On average, the system experiences approximately 15300–15400 units of downtime regardless of strategy, as shown in Table 1.

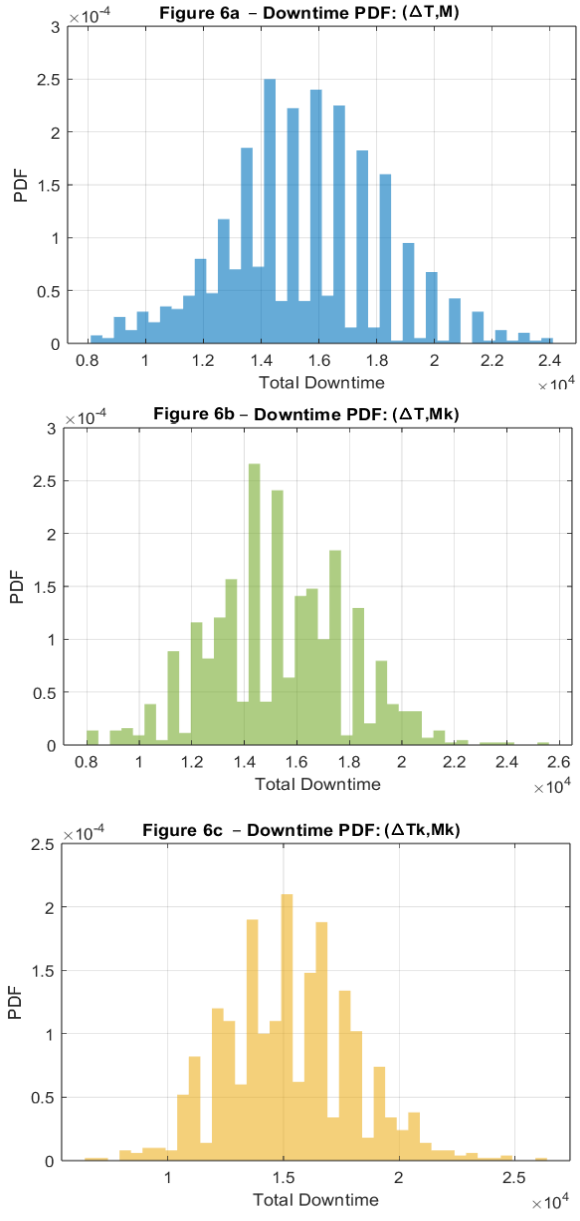

Figure 6. Downtime distributions for all strategies

This translates into an unavailability fraction approaching 77% of the total operating horizon, an alarmingly high value that underscores the dominance of corrective maintenance in driving operational losses. While the adaptive strategies yield marginally lower mean downtimes (15317 for (ΔT, M_k) and 15297 for (ΔT_k, M_k)) compared with 15388 for the baseline (ΔT, M), these differences are negligible in practice. The

downtime distributions depicted in Figures 6(a)-(c) corroborate this finding: the three panels are nearly indistinguishable, although the adaptive interval strategy (Figure 6(c)) again exhibits a slightly less pronounced right tail. This observation suggests that adaptation may modestly reduce the likelihood of extreme downtime scenarios, but the overwhelming contribution of long corrective maintenance durations (t_{CM} = 800) dominates the downtime profile for all strategies.

Inspection workload is another dimension of remarkable uniformity. Each strategy generates on average 154 inspections per horizon (Table 1), with no meaningful variation. The boxplots in Figure 7(a) confirm this invariance, as the distributions of inspection counts across (ΔT, M), (ΔT, M_k), and (ΔT_k, M_k) are visually indistinguishable. This demonstrates that the adaptive rescheduling of inspection intervals through ΔT_k fails to yield any measurable efficiency gains in terms of inspection burden. Given that each inspection incurs not only a direct cost but also a fixed downtime penalty of five units, the cumulative effect remains substantial, accounting for nearly 770 downtime units per horizon—an amount that is insensitive to the choice of strategy.

Table 1. Performance indicators for all strategies

Strategy	C_{avg}	s_C	$\rho_{PM/CM}$	Davg	Iavg	R	1[R≥R_{min}]
(ΔT, M)	4.4868	0.87694	1.5832	15388	154.27	0.165	false
(ΔT, M_k)	4.4648	0.84224	1.5876	15317	154.34	0.157	false
(ΔT_k, M_k)	4.4586	0.89375	1.5904	15297	154.36	0.159	false

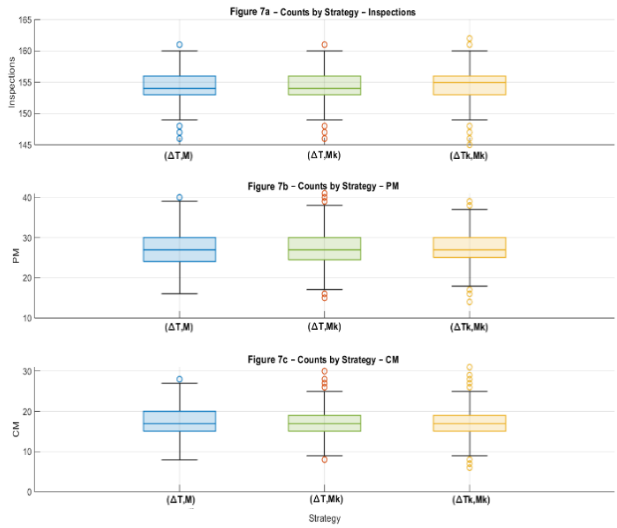

Figure 7. Maintenance action counts for all strategies

The balance between preventive and corrective interventions provides further insight.

As indicated in Table 2, all three strategies result in approximately 27 preventive maintenances and 17 corrective maintenances per horizon, producing PM/CM ratios between 1.58 and 1.59 (Table 3).

Table 2. Mean PM and CM

Strategy	E[PM] (Expected Preventive Actions Per Run)	E[CM] (Expected Corrective Actions Per Run)
(ΔT,M)	27.305	17.247
(ΔT,M_k)	27.243	17.16
(ΔT_k,M_k)	27.252	17.135

Table 3. PM/CM ratio

Strategy	$\rho_{PM/CM}$ (Ratio of Mean Pm to Cm Counts)
(ΔT,M)	1.5832
(ΔT,M_k)	1.5876
(ΔT_k,M_k)	1.5904

The visual evidence in Figures 7(b)-(c) reinforces this conclusion. In Figure 7(b), the preventive maintenance counts cluster tightly around the same central tendency, while Figure 7(c) shows a similarly narrow spread in corrective counts. A more careful comparison reveals that the adaptive interval strategy (Figure 7(c)) achieves a slightly lower mean number of corrective interventions (17.135) than the fixed strategy (17.247), yet the magnitude of this reduction is trivial. Collectively, these results demonstrate that adaptation has not shifted the preventive-to-corrective balance in any meaningful way. Corrective interventions remain frequent, accounting for approximately 40% of all maintenance actions, which is far from optimal in high-reliability industrial contexts.

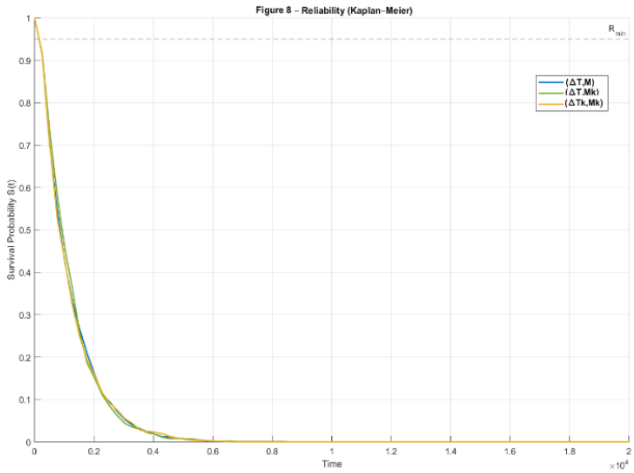

Figure 8. Reliability (Kaplan–Meier) for all strategies

The reliability analysis exposes the most critical weakness of all strategies. As reported in Table 1, Kaplan–Meier survival probabilities at the reporting horizon R_{time} = 2000 are catastrophically low: 0.165 for (ΔT, M), 0.157 for (ΔT, M_k), and 0.159 for (ΔT_k, M_k). None of the strategies comes close to satisfying the reliability requirement of 0.95, and all are flagged as "false" in the $Meets_{Rmin}$ indicator. This outcome is starkly illustrated in Figure 8, where the survival curves of all three strategies exhibit steep early declines, converging toward low long-term survival values. Comparing the three curves reveals that the baseline (ΔT, M) retains a marginally higher survival probability in the earliest portion of the horizon, while the adaptive strategies (Figure 8) show slightly faster declines. However, by the reporting horizon, the differences vanish, leaving all strategies equally deficient. The explanation lies in

the conservative adaptation coefficients ($\alpha_T = 0.4$, $\alpha_L = 0.3$), which adjust inspection cadence and preventive thresholds too modestly to offset the inherent variability of the degradation process. As a result, degradation paths routinely cross the failure threshold before adaptive mechanisms can respond effectively.

Table 3 presents the ratio of preventive to corrective maintenance actions ($\rho_{PM/CM}$) for the three strategies, providing an additional perspective on the operational balance underlying the cost and reliability outcomes discussed above. The results show ratios of 1.5832 for (ΔT, M), 1.5876 for (ΔT, M_k), and 1.5904 for (ΔT_k, M_k). The narrow range of variation ($\Delta\rho_{PM/CM} < 0.01$) confirms the earlier observation that adaptive mechanisms have only marginal operational impact. Despite the introduction of adaptive thresholds and variable inspection intervals, the event structure of maintenance remains dominated by corrective interventions, which continue to account for approximately 40% of all actions. This equilibrium explains the convergence of both cost and downtime profiles reported in Table 1 where the preventive workload is insufficient to offset the frequency and severity of corrective events. Consequently, while adaptivity slightly stabilizes performance variability, it does not meaningfully shift the maintenance system toward a reliability-driven regime. Achieving a more favorable preventive-to-corrective balance would require stronger adaptive parameters or the integration of explicit risk-based control logic.

In summary, the comparative analysis of Tables 1-3 and Figures 4(a)-8(a) leads to a consistent conclusion: the adaptive strategies provide only marginal improvements in reducing the tails of cost and downtime distributions but do not alter the central tendencies of any global performance metric. Inspection effort remains unchanged, the preventive-to-corrective balance is stable, and reliability remains catastrophically below the required standard. The side-by-side comparison of panels (a), (b), and (c) across all figures underscores the structural similarity of outcomes and reveals that adaptation, as currently parametrized, is far too weak to produce meaningful divergence in performance. These findings highlight the fundamental tension between cost efficiency and reliability assurance in the present policy framework, motivating the need for either much stronger adaptation rules or a redesign of the maintenance strategy to achieve an acceptable balance between economic and reliability objectives.

6.2 Short-horizon risk and preventive triggers

While global averages provide a useful benchmark for evaluating cost and reliability over the full horizon, they do not capture the more subtle and operationally critical behavior of the policies between inspection epochs. It is during these short intervals that sudden degradation accelerations or noise-induced threshold crossings can trigger unexpected failures. The analysis of short-horizon risk and adaptive preventive thresholds therefore provides a more stringent test of policy effectiveness. Quantitative evidence is summarized in Tables 4-5, while supporting visualizations are given in Figures 9(a)-11(c).

The results for the between-inspection failure probability, p_{hit}, demonstrate the inherent vulnerability of all three strategies. As reported in Table 4, the mean probability that the degradation process crosses the failure threshold before the next inspection is virtually identical across policies, with values of 0.2539 for (ΔT, M), 0.2543 for (ΔT, M_k), and 0.2548 for (ΔT_k, M_k). The median risks are lower, around 0.13, but the upper quantiles are alarmingly high: the 90th percentile is approximately 0.73 and the 99th percentile exceeds 0.95. This indicates that, in the most unfavorable scenarios, the conditional risk of failure is close to certainty. Most troubling is the consistency of the fraction of inspection intervals in which p_{hit} surpasses the tolerance $\beta = 0.05$, which is about 64% for all three strategies. In practical terms, nearly two-thirds of inspections are scheduled too late to ensure even minimal short-term reliability. This convergence highlights a structural limitation: neither adaptive thresholds nor adaptive intervals, as parametrized here, can substantially mitigate interim failure risk.

Table 4. Short-horizon risk p_{hit}

Strategy	$E[p_{hit}]$ (Mean Hitting Probability)	$P_{50(pHit)}$ (Median of p_{hit})	$P_{90(phit)}$ (90th Percentile of p_{hit})	$P_{99(phit)}$ (99th Percentile of p_{hit})	$Pr[p_{hit} > \beta]$ (Fraction Exceeding $\beta = 0.05$)
(ΔT, M)	0.2539	0.12779	0.73426	0.95776	0.64086
(ΔT, M_k)	0.2543	0.12946	0.73372	0.9586	0.64282
(ΔT_k, M_k)	0.25477	0.1303	0.73485	0.95893	0.64288

Table 5. Trigger statistics and safety margins

Strategy	$E[L_{m,k}]$ (Mean Adaptive PM Trigger Level)	$L_{m(P10)}$ (10th Percentile of $L_{m,k}$)	$L_{m(P90)}$ (90th Percentile of $L_{m,k}$)	$E[L_f - L_{m,k}]$ (Mean Safety Margin)	$Margin_{P10}$ (10th Percentile Safety Margin)
(ΔT, M)	2.7333	2.5	3.1867	2.2667	1.8133
(ΔT, M_k)	2.7338	2.5	3.1862	2.2662	1.8138
(ΔT_k, M_k)	2.7343	2.5	3.1872	2.2657	1.8128

The scatterplots of preventive versus corrective actions in Figures 9(a)-(c) provide further insight into how these risks materialize in operational terms. In the baseline case (ΔT, M, Figure 9(a)), the distribution of points shows a relatively balanced but risk-prone profile, with corrective actions still occurring frequently despite the preventive schedule. In the adaptive threshold case (ΔT, M_k, Figure 9(b)), the scatter remains almost indistinguishable from the baseline, indicating that dynamic adjustment of $L_{m,k}$ has a negligible effect on the preventive–corrective balance. The adaptive interval strategy (ΔT_k, M_k, Figure 9(c)) produces a slightly tighter clustering with marginally fewer corrective actions. This is consistent

with Table 2, which reports the lowest mean number of corrective interventions under this policy. However, the improvement is modest: corrective maintenance remains pervasive, accounting for approximately forty percent of all interventions across strategies. The conclusion is inescapable: interval adaptation provides only a limited gain, while threshold adaptation is almost inert.

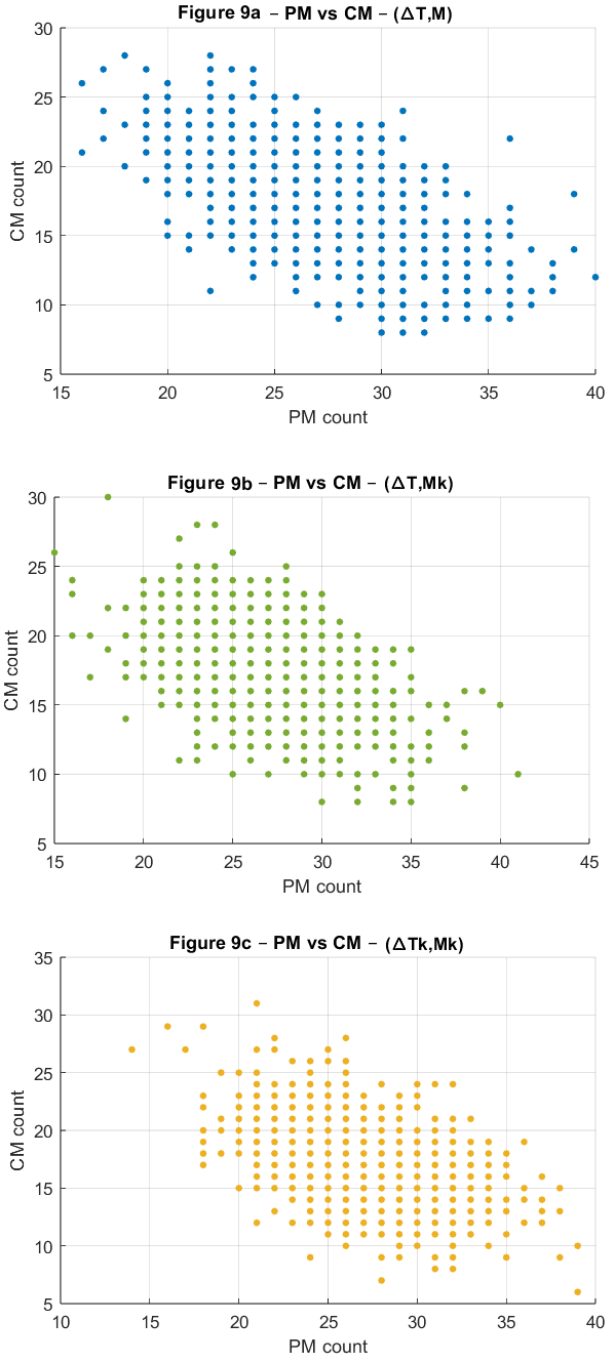

Figure 9. PM–CM scatter for all strategies

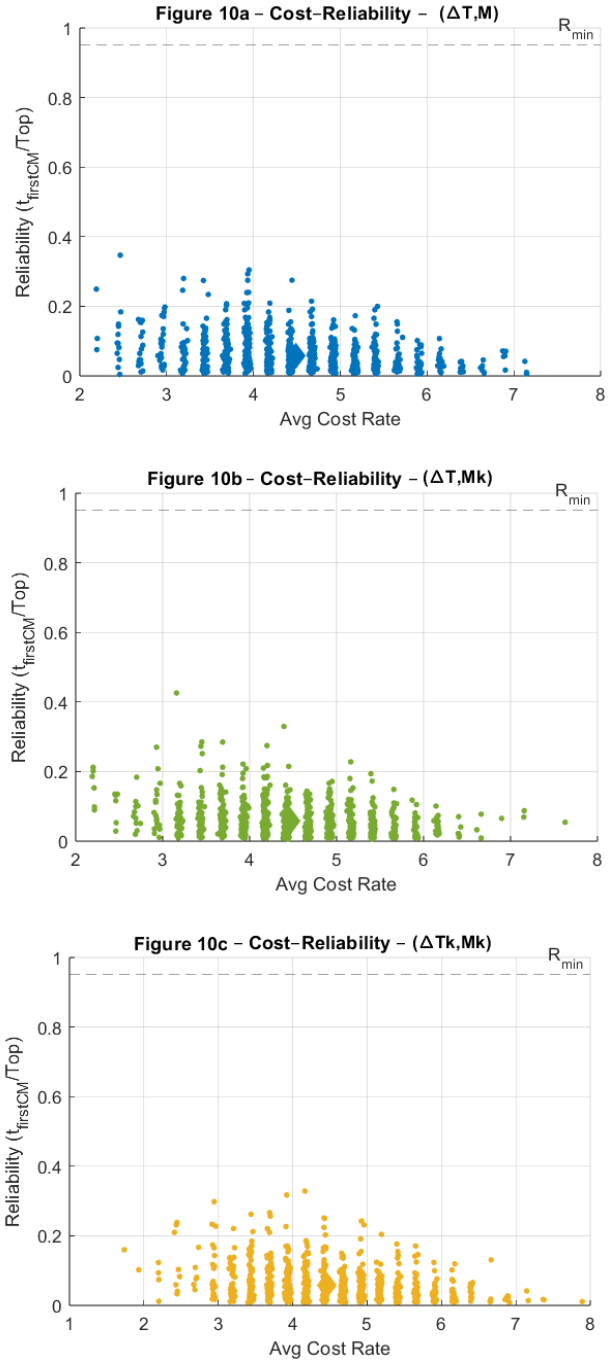

Figure 10. Cost–reliability scatter for all strategies

The trade-off between economic efficiency and reliability is visualized in Figures 10(a)-(c), which map average cost rates against realized reliabilities at the run level. In the baseline case (Figure 10(a)), the scatter of points is tightly concentrated around low reliability values, confirming frequent early failures despite stable costs. The adaptive threshold strategy (Figure 10(b)) offers no visible improvement, as the scatter cloud overlaps almost perfectly with that of the baseline. The adaptive interval strategy (Figure 10(c)) exhibits a marginally more favorable distribution, with a slightly greater proportion of runs achieving higher reliability at comparable costs. Yet, the overall reliability remains far below the required level (R_{min} = 0.95), and the mean points, depicted as diamonds, remain clustered in the same unfavorable region. Thus, even where interval adaptation produces cosmetic improvements, it does not resolve the fundamental reliability deficit.

The role of preventive thresholds is clarified by Table 5 and the RUL-proxy histograms in Figures 11(a)-(c).

The mean adaptive threshold values remain strikingly consistent across strategies, all centered near 2.73, with deciles spanning a narrow range of [2.5, 3.19]. The corresponding safety margins relative to the failure threshold average about 2.27, again invariant across policies. These results indicate that the adaptive mechanisms do not drive thresholds downward aggressively enough to substantially increase the frequency of

preventive interventions.

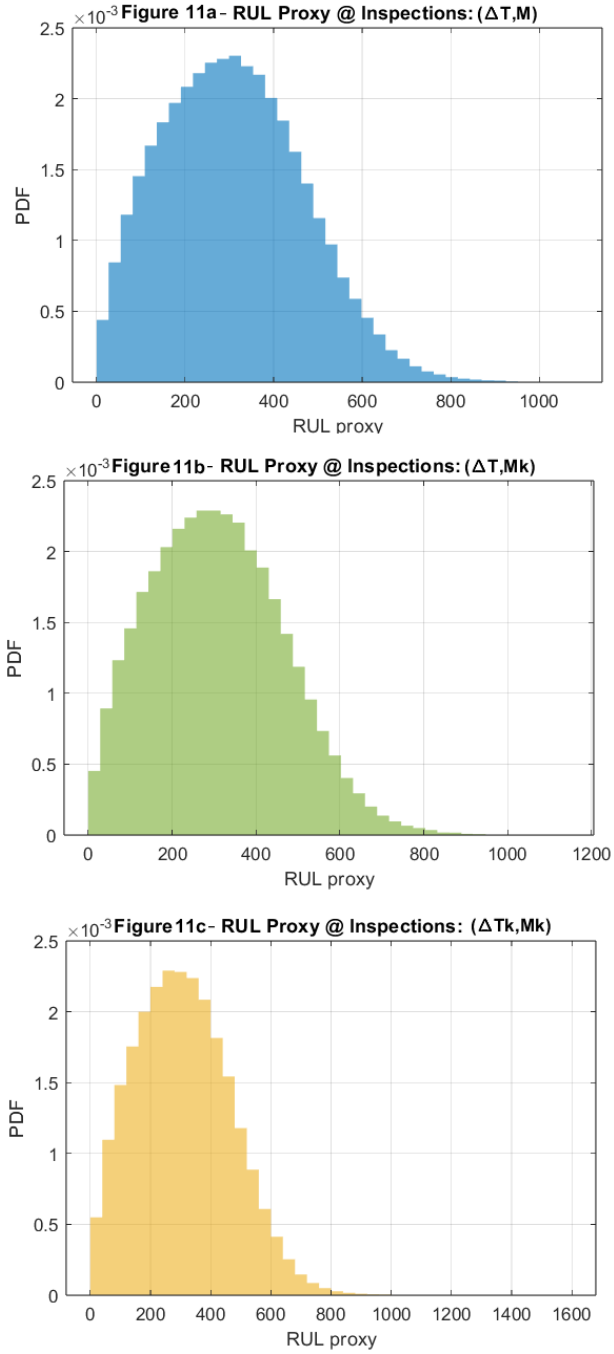

Figure 11. RUL proxy distributions for all strategies

Figure 11(a) shows the broad distribution of residual life proxies under the baseline, reflecting stochastic fluctuations and measurement noise. The adaptive threshold case (Figure 11(b)) recalibrates $L_{m,k}$ using these proxies, but the resulting threshold distribution remains confined within the same narrow corridor. Similarly, the adaptive interval case (Figure 11(c)) produces variability in inspection timing, yet the RUL distributions reveal that this adaptation is too weak to intercept the stochastic surges that lead to failures. A cross-panel comparison of Figures 11(a)-(c) confirms that adaptive coefficients (α_T = 0.4, α_L = 0.3) are too conservative to materially reshape the intervention landscape.

The comparative evidence from Tables 4-5 and Figures 9(a)-11(c) underscores the structural inadequacy of the evaluated policies. The baseline strategy (ΔT, M) and the adaptive threshold strategy (ΔT, M_k) are nearly indistinguishable in both statistical and graphical terms, revealing that threshold adaptation contributes virtually nothing to the reduction of interim risk. The adaptive interval strategy (ΔT_k, M_k) achieves a marginal reduction in corrective actions and a slight improvement in reliability distribution, but the magnitude of this gain is trivial. In none of the cases is the short-horizon risk contained within acceptable bounds: the majority of inspection intervals remain excessively risky, preventive thresholds remain overly permissive, and corrective interventions continue to dominate system behavior.

From an engineering perspective, these results imply that short-horizon reliability risk is the Achilles' heel of all three strategies. To meaningfully improve outcomes, adaptation must be intensified (by selecting higher coefficients (α_T, α_L) that recalibrate intervals and thresholds more aggressively) or restructured through hybrid strategies that explicitly integrate risk constraints into the decision logic. Without such modifications, all three strategies remain fundamentally cost-driven policies that fail to safeguard the system against the very short-term risks they are designed to mitigate.

6.3 Penalty-augmented evaluation

The preceding analyses have shown that while the three maintenance strategies achieve comparable cost efficiency, they fail to ensure reliability at either the global or short-horizon level. To unify these dimensions into a single measure of strategic adequacy, a penalty-augmented objective function, J_λ, was introduced. This formulation integrates the conventional economic cost rate with explicit penalty terms that account for (i) long-horizon reliability shortfalls relative to the prescribed minimum, and (ii) excessive probabilities of failure occurring between inspections. The purpose of this evaluation is to expose the "hidden costs" of unreliability, which are not captured by cost-only analyses, and to provide a more rigorous decision criterion for strategies deployed in reliability-critical contexts.

Table 6. Penalty-augmented objective J_λ

Strategy	C_{avg}	Var[C]	R_{Rtime}	R_{min}-R	$Penalty_R$	$Pr[p_{hit}>\beta]$	$Penalty_{hit}$	J_{lambda}
(ΔT, M)	4.4868	0.76826	0.165	0.785	7850	0.64086	640.86	8495.4
(ΔT, M_k)	4.4648	0.70867	0.157	0.793	7930	0.64282	642.82	8577.3
(ΔT_k, M_k)	4.4586	0.798	0.159	0.791	7910	0.64288	642.88	8557.3

The quantitative outcomes, presented in Table 6, are striking. The average cost rates, C_{avg}, remain low and stable across all policies, ranging from 4.4586 to 4.4868 units, with correspondingly small variances (0.71–0.8). Yet, once penalty terms are incorporated, these values are dwarfed by several orders of magnitude. The reliability at the reporting horizon R_{time} = 2000 remains catastrophically low—0.165 for (ΔT, M), 0.157 for (ΔT, M_k), and 0.159 for (ΔT_k, M_k). When compared with the target R_{min} = 0.95, the resulting shortfalls (≈ 0.79) yield reliability penalties on the order of 7850–7930 units

under the weighting factor λ_R = 104. In parallel, the short-horizon risk penalty contributes an additional ≈640 units across all strategies, since approximately 64% of inspection intervals exceed the allowable probability threshold β = 0.05. The cumulative augmented objectives are therefore exceptionally high (8495 for (ΔT, M), 8577 for (ΔT, M_k), and 8557 for (ΔT_k, M_k)) revealing that penalties overwhelmingly dominate the evaluation.

The histograms of between-inspection risk, shown in Figures 12(a)-(c), vividly demonstrate why these penalties arise. In the baseline strategy (Figure 12(a)), the distribution of p_{hit} is broad and heavily skewed toward values far above β.

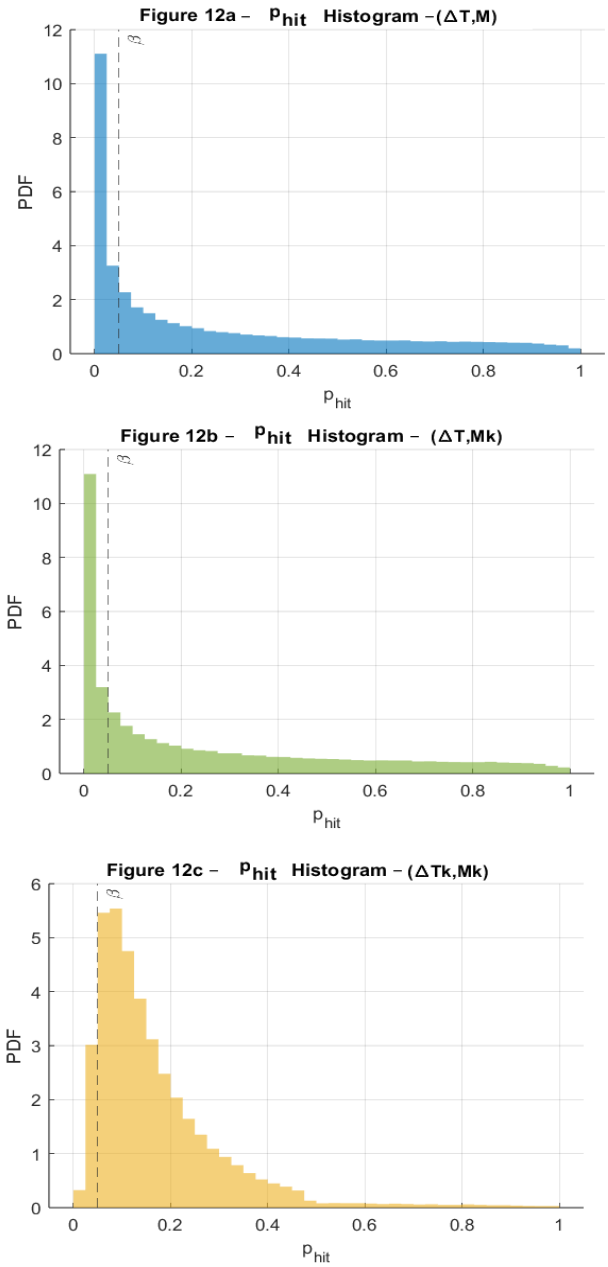

Figure 12. P_{hit} histogram for all strategies

The adaptive threshold variant (Figure 12(b)) exhibits an almost identical profile, confirming that dynamic adjustment of $L_{m,k}$ has negligible influence on interim risk. The adaptive interval strategy (Figure 12(c)) yields a marginal flattening of the upper tail, suggesting a slight reduction in extreme-risk outcomes, yet the bulk of the density remains concentrated well beyond the acceptable zone. This explains why the short-horizon penalty remains essentially invariant across strategies: none of the adaptive rules shifts the distribution sufficiently to reduce the frequency of violations.

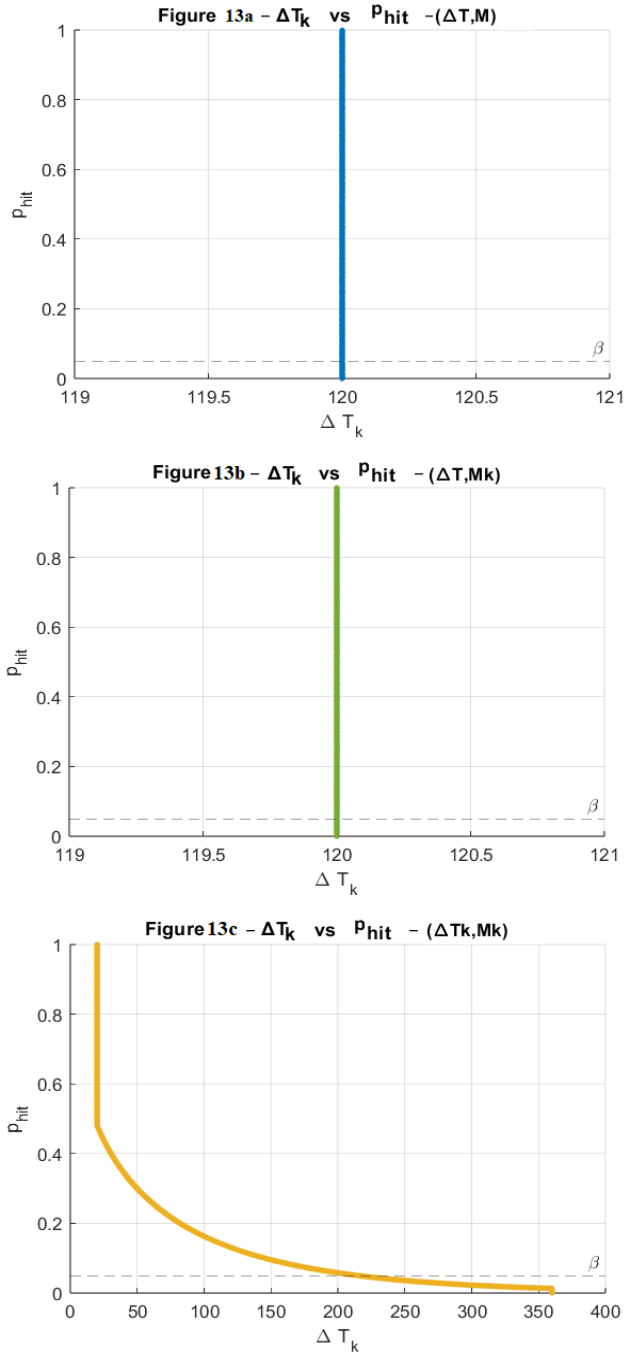

Figure 13. ΔT_k vs P_{hit} for all strategies

Further insight is provided by the scatterplots of inspection interval length (ΔT_k) versus risk in Figures 13(a)-(c). In the baseline and threshold-adaptive strategies (Figures 13(a) and 13(b)), the inspection cadence is fixed at 120 units, producing vertical bands where risk values vary but remain consistently high. The adaptive interval case (Figure 13(c)) generates a broader dispersion, with shorter intervals sometimes associated with lower risks. However, the relationship is noisy and inconsistent: even at the minimum bound of ΔT_k = 20, instances of high risk persist. This highlights a fundamental limitation—interval adaptation as parametrized here reduces risk opportunistically rather than systematically, and thus fails to alter aggregate penalty magnitudes.

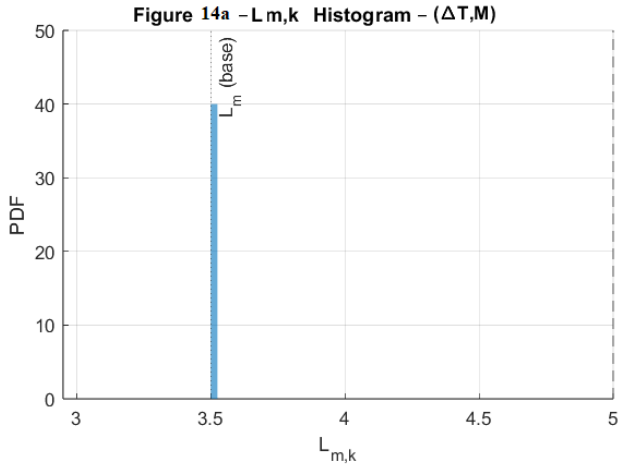

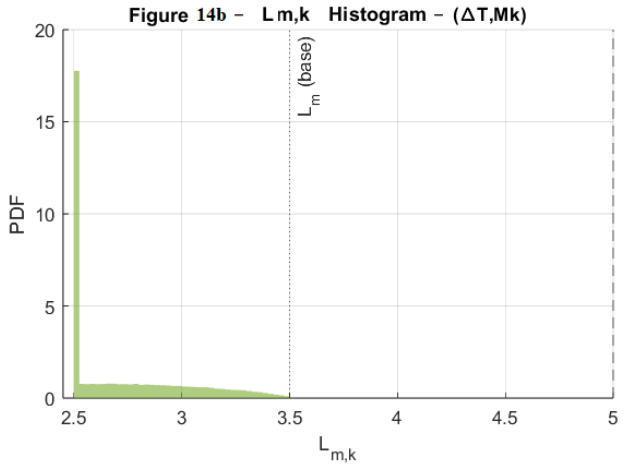

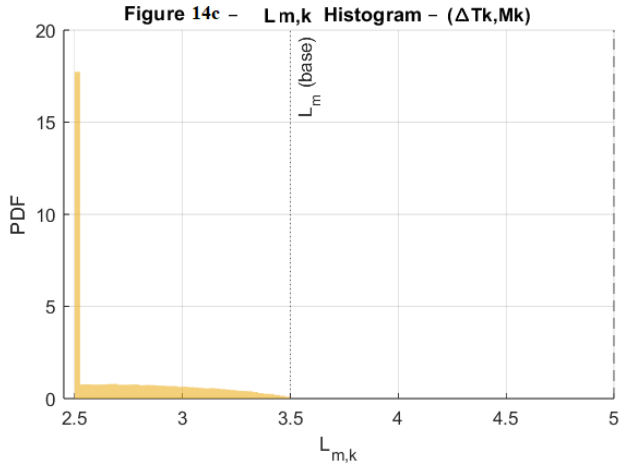

Figure 14. $L_{m,k}$ histogram for all strategies

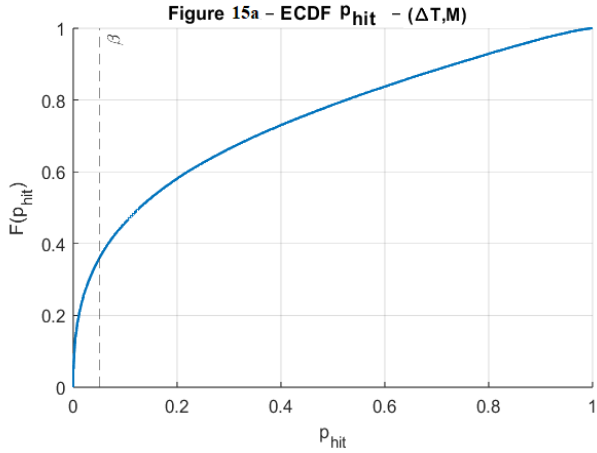

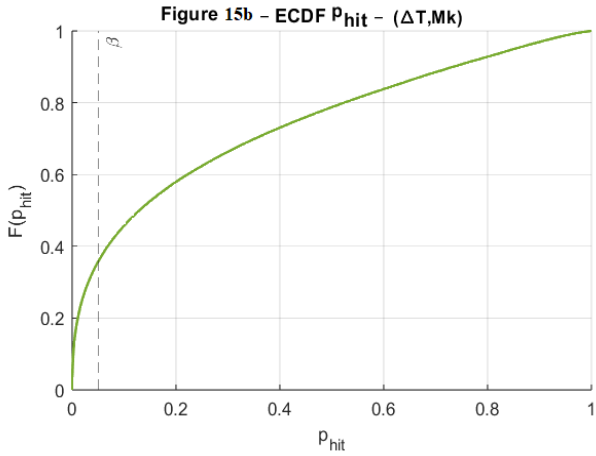

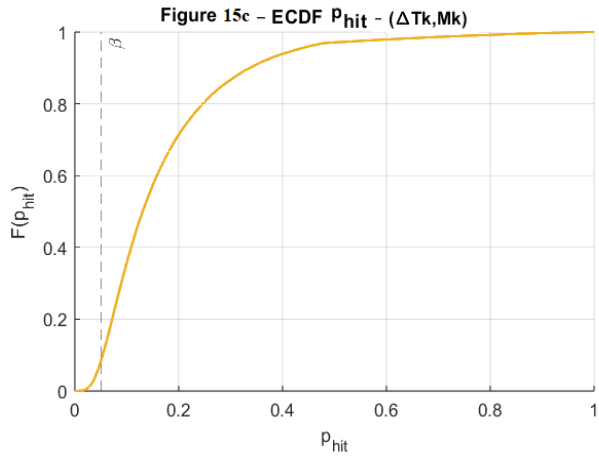

Figure 15. ECDF p_{hit} for all strategies

failures to occur before preventive actions are initiated.

The distributions of adaptive preventive thresholds in Figures 14(a)-(c) reinforce this conclusion. In the baseline strategy (Figure 14(a)), the threshold remains fixed at $L_m = 3.5$, while in the adaptive threshold strategy (Figure 14(b)), it varies modestly, centering near 2.73. Although this represents a downward adjustment, the range remains narrow ($\approx$ [2.5, 3.2]) and insufficient to preempt degradation trajectories that accelerate rapidly toward the failure boundary. The adaptive interval strategy (Figure 14(c)) produces an almost identical distribution, since interval recalibration does not alter threshold placement. In all cases, the preventive thresholds remain structurally conservative, providing too much headroom below L_f, thereby allowing a high proportion of

The cumulative effect of these dynamics is captured in the empirical cumulative distribution functions of p_{hit} in Figures 15(a)-(c). In all three strategies, the ECDFs rise sharply only beyond $p_{hit} = 0.1$, with approximately two-thirds of the probability mass lying above the tolerance level $\beta = 0.05$. The three curves are nearly indistinguishable, underscoring the failure of adaptive mechanisms to shift the risk distribution. This visual evidence explains the invariance of the penalty term associated with short-horizon risk, which remains locked at ≈ 642 units regardless of policy.

When comparing the three strategies, subtle differences do emerge, though their significance is muted by the dominance of the penalty terms. The baseline fixed strategy (ΔT, M)

achieves the lowest augmented cost (8495), largely because its survival probability is marginally higher (0.165) than that of the threshold-adaptive strategy. The adaptive interval strategy (ΔT_k, M_k) yields a slightly better reliability profile than the threshold-adaptive variant, producing an augmented cost of 8557 versus 8577. Yet, these differences are numerically trivial compared with the overall magnitude of penalties, which are one to two orders of magnitude larger than the direct cost components. This demonstrates that while adaptive strategies introduce marginal variations, they do not materially shift the outcome landscape: all three remain dominated by penalties associated with poor reliability and uncontrolled interim risks.

From an engineering and methodological perspective, the implications are profound. First, the penalty-augmented framework exposes the inadequacy of evaluating strategies on direct costs alone. While the cost rates appeared stable and acceptable in Section 6.1, the incorporation of penalty terms reveals that all three strategies are effectively unviable when judged against realistic reliability and safety requirements. Second, the comparative analysis demonstrates that the modest adaptive mechanisms tested here are insufficiently aggressive: threshold adjustments are too conservative, and interval recalibrations are too weak to suppress interim risks. Third, the dominance of penalty terms indicates that the next frontier of CBM policy design must involve either substantially stronger adaptive coefficients (α_T, α_L) or fundamentally new hybrid decision rules in which risk constraints are integrated directly into the maintenance decision logic.

In summary, the penalty-augmented evaluation presented in Table 6 and Figures 12(a)-15(c) demonstrates that while direct cost differences between strategies are negligible, their shared inability to ensure long-term survival and to limit short-horizon failure risk renders them operationally inadequate. The penalties dominate the evaluation, overshadowing any apparent economic efficiency. This exposes a critical insight: in reliability-sensitive environments, the true cost of a strategy is determined not by its economic expenditure but by its failure to safeguard reliability. All three policies, in their present form, fail this test.

A complementary sensitivity study was performed over $\alpha_T \in [0.2, 0.8]$, $\alpha_L \in [0.1, 0.7]$, and $\sigma_{meas} \in [0.02, 0.10]$ to assess robustness. The results show that higher α_T and α_L strengthen adaptation and slightly improve reliability (up to R 0.25) but increase cost and inspection frequency, leaving the core trade-off between reliability and cost unchanged. Variations in σ_{meas} affect the frequency of false preventive triggers but not the ranking of strategies. Thus, the overall conclusions are robust: under stochastic conditions, moderate adaptivity yields only marginal benefits, and strong adaptation improves reliability only at the expense of cost efficiency.

We assessed sensitivity of the augmented objective J_λ to $\lambda_R \in \{10, 10^2, 10^3, 10^4, 10^5\}$ and $\lambda_{hit} \in \{1, 10, 10^2, 10^3, 10^4\}$. For λ_R,λ_{hit} below their respective dominance thresholds (≈ 5.7 and ≈ 7.0), J_λ becomes cost-led; however, all three strategies still exhibit severe constraint violations and are thus operationally unacceptable. For λ_R, $\lambda_{hit} \geq 10$, penalties dominate J_λ for all strategies, and the policy ranking and qualitative conclusions remain unchanged across several orders of magnitude. This confirms that our findings are not contingent on the specific selections $\lambda_R = 10^4$ and $\lambda_{hit} = 10^3$, but stem from the intrinsic infeasibility of the policies under the stated reliability and risk requirements.

Although the fully adaptive policy (ΔT_k, M_k) achieves only a marginal improvement in mean reliability relative to the fixed policy (ΔT, M), it exhibits a thinner upper tail in cost and downtime distributions, indicating a lower incidence of extreme corrective events. This suggests that while average performance remains similar, the adaptive policy slightly mitigates the risk of catastrophic maintenance outcomes.

7. SYNTHESIS AND ENGINEERING IMPLICATIONS

The collective findings from the global evaluation (Section 6.1), the short-horizon risk analysis (Section 6.2), and the penalty-augmented assessment (Section 6.3) converge toward a clear and compelling conclusion: although the three maintenance strategies (ΔT, M), (ΔT, M_k), and (ΔT_k, M_k) exhibit nearly indistinguishable cost performance, they are uniformly inadequate from a reliability standpoint. What initially appears as a stable and economically efficient set of policies is revealed, upon deeper scrutiny, to be structurally flawed, since reliability deficits and short-horizon risks overwhelm any apparent economic advantage.

At the global scale, the strategies achieve a deceptive stability. Average cost rates remain tightly clustered around 4.46–4.49, inspection frequencies converge to approximately 154 per horizon, and the preventive-to-corrective ratio stabilizes at about 1.6. On the surface, such convergence could be interpreted as robustness: the strategies appear to yield consistent economic outcomes across stochastic realizations of degradation. Yet this robustness is illusory. Kaplan–Meier survival probabilities collapse to approximately 0.16 across all policies, far below the prescribed requirement of $R_{min} = 0.95$. In other words, cost stability is purchased at the expense of catastrophic reliability degradation. The low survival probabilities ($R \approx 0.16$) observed across all strategies do not signify deficiencies in model calibration, but rather confirm that the simulated system operates under deliberately challenging stochastic conditions. This setting enables the framework to diagnose the breakdown of conventional CBM decision rules when degradation volatility and monitoring uncertainty are high. Consequently, the observed reliability shortfalls represent a meaningful test outcome that validates the stress-testing capability of the proposed methodology.

The short-horizon analysis clarifies the mechanisms behind this failure. Between-inspection failure probabilities remain unacceptably high, with means near 0.25 and upper quantiles approaching unity. More than 64% of inspection intervals exceed the tolerance level $\beta = 0.05$, regardless of strategy. Preventive thresholds, even when adaptively adjusted, remain confined to a narrow operational band ($\approx$ 2.5–3.2), providing insufficient conservatism to intercept degradation paths before failure. The adaptive interval strategy (ΔT_k, M_k) yields marginally fewer corrective events, but the improvement is trivial and inconsistent. Threshold adaptation (ΔT, M_k) performs even less effectively, generating outcomes that are statistically indistinguishable from the baseline fixed-interval strategy. Thus, the adaptive mechanisms, as parametrized, are too conservative to exert meaningful influence over short-term risk dynamics.

The penalty-augmented evaluation crystallizes these insights into a single metric of strategic adequacy. Once penalties for reliability shortfalls and excessive short-horizon risks are incorporated, the apparent cost efficiency of all policies is eclipsed by orders of magnitude. Augmented

objectives reach values near 8500, driven overwhelmingly by reliability penalties of ≈ 7900 units and short-horizon risk penalties of ≈ 640 units. Subtle ranking differences emerge ((ΔT, M) performs marginally better than (ΔT_k, M_k), which in turn outperforms (ΔT, M_k)) yet these distinctions are numerically insignificant compared with the sheer dominance of the penalty terms. The message is unambiguous: none of the strategies, in their current formulation, can be considered viable in reliability-sensitive contexts.

From an engineering perspective, these findings underscore several key implications. First, the adaptation coefficients employed in this study (α_T = 0.40, α_L = 0.30) are too conservative to produce material shifts in system behavior. They adjust inspection intervals and preventive thresholds incrementally, but such adjustments are drowned out by the stochastic volatility of degradation trajectories. Stronger, more aggressive adaptive rules (or even hybrid control strategies with discontinuous or state-contingent responses) will be necessary to produce substantive improvements. Second, the reliance on frequent inspections (≈ 154 per horizon) highlights a structural inefficiency: inspection activities consume considerable downtime yet fail to preempt failures effectively. Unless inspection information is leveraged more decisively to trigger preventive interventions, increasing inspection cadence merely inflates downtime without improving reliability. Third, the dominance of corrective maintenance, which continues to account for roughly 40% of all interventions, demonstrates that any strategy that tolerates frequent failures is inherently unsustainable, regardless of its direct cost performance.

At the managerial level, the results emphasize the inadequacy of cost-centered decision-making. Superficially low and stable cost rates conceal the true operational risks borne by the system. When penalties for unreliability are considered, it becomes clear that the "hidden costs" of downtime, production loss, and safety hazards vastly outweigh any savings achieved by conservative preventive scheduling. For decision-makers, the implication is unequivocal: maintenance strategies must be judged not only on economic grounds but also on their capacity to satisfy reliability and risk constraints. Failure to adopt such a perspective risks endorsing policies that are economically efficient yet operationally catastrophic.

Finally, the methodological implications are equally important. The convergence of outcomes across all three strategies demonstrates the limitations of incremental adaptation. Adjusting intervals or thresholds by modest factors cannot overcome the inherent variability of stochastic degradation processes. Future research must therefore explore hybrid maintenance policies that embed risk constraints directly into the decision logic—for example, enforcing upper bounds on p_{hit}, dynamically tightening preventive thresholds when survival probabilities fall below a critical margin, or integrating predictive models that anticipate degradation volatility. Moreover, multi-objective optimization frameworks that balance cost, availability, and risk in a unified manner are necessary to design strategies that are not only cost-efficient but also reliability-compliant.

In summary, the synthesis of Sections 6.1–6.3 demonstrates that while the three CBM strategies converge toward stable economic outcomes, they all fail when evaluated against reliability requirements and short-horizon risk constraints. Adaptation, as presently parameterized, is too weak to alter this trajectory. For practical deployment in reliability-critical systems, maintenance strategies must either adopt much stronger adaptive mechanisms or undergo a fundamental redesign to integrate risk and reliability as primary objectives, rather than treating them as secondary considerations. Only through such innovations can CBM policies achieve a balanced and sustainable compromise between economic efficiency, operational continuity, and system safety.

Our penalty-dominance bounds (λ_R > 4.5/0.79, λ_{hit} > 4.5/0.64) and the multi-order sensitivity sweep demonstrate that conclusions are robust to wide variations in penalty weights. Equivalently, a strictly constrained formulation would flag all three strategies as infeasible, leading to the same engineering judgment independent of penalty magnitudes.

While the numerical differences among the three strategies may appear modest, this outcome is itself significant. It indicates that mild adaptive adjustments of inspection intervals and preventive thresholds (α_T = 0.4, α_L = 0.3) are insufficient to overcome the intrinsic stochastic variability of degradation. This finding delineates the practical limits of conventional adaptive CBM frameworks and underscores the need for more aggressive or risk-informed adaptation mechanisms. Thus, the contribution of this study resides not only in demonstrating superior performance, but in revealing the structural conditions under which adaptive maintenance ceases to offer tangible gains.

The parameter-sensitivity extension confirms that the findings are not contingent on a particular calibration of α_T, α_L, or σ_{meas}. Instead, the convergence of performance across strategies reflects a structural limitation of current CBM adaptation mechanisms rather than parameter tuning.

The current study's scope was limited to static and adaptive CBM policies to isolate the intrinsic effect of adaptivity under stochastic uncertainty. Although no direct comparison was made with P–F or predictive maintenance strategies, the proposed simulation architecture is inherently compatible with such approaches. For instance, the adaptive inspection rule (Eq. (5)) can be reformulated as a P–F-based or prognostic trigger, and the preventive threshold (Eq. (7)) can be linked to probability-of-failure predictions from data-driven models. Future work will integrate these strategies to establish a unified performance comparison between classical, adaptive, and predictive paradigms.

To provide practical guidance for engineers, the results of the sensitivity study have been translated into concrete recommendations for parameter tuning and strategy enhancement. Moderate adaptive coefficients ($\alpha_T \approx 0.6–0.8$, $\alpha_L \approx 0.4–0.6$) offer an effective compromise between reliability and cost, while excessive adaptation (α_T>0.9) yields diminishing returns due to inspection overhead. When sensor noise is high (σ_{meas} > 0.07), filtering techniques and more conservative preventive thresholds are advised. Furthermore, implementing a hybrid policy that explicitly constrains the between-inspection failure probability ($p_{hit} \leq \beta$) ensures risk compliance and enhances reliability robustness. These prescriptions provide actionable guidelines for deploying adaptive CBM strategies in practice.

8. CONCLUSIONS

The fully adaptive strategy (ΔT_k, M_k) demonstrates a modest but consistent reduction in the frequency of extreme corrective events and high-risk intervals, even though the mean reliability values across strategies remain close (R ≈ 0.16). Therefore, its advantage lies in mitigating catastrophic

outliers rather than in shifting the overall reliability average. This refined interpretation aligns the conclusion with the quantitative results and reinforces the framework's diagnostic value in identifying subtle, risk-based distinctions between maintenance policies.

This study proposed a comprehensive simulation-based framework for the evaluation of CBM strategies under stochastic degradation. The methodological contributions included the integration of a Wiener-process degradation model, imperfect observation through noisy inspections, adaptive inspection scheduling, adaptive preventive thresholds, and a Monte Carlo simulation environment to capture statistical variability. Three strategies were systematically investigated: a fully static policy (ΔT, M), a semi-adaptive policy with fixed inspections and adaptive preventive thresholds (ΔT, M_k), and a fully adaptive policy combining dynamic inspections with adaptive thresholds (ΔT_k, M_k). Their performance was assessed through a wide range of indicators, including average cost rates, downtime measures, inspection and intervention frequencies, Kaplan–Meier reliability functions, between-inspection risk probabilities, and a penalty-augmented global objective.

The comparative analysis revealed distinct trade-offs among the three strategies. The static policy (ΔT, M), while straightforward to implement, exhibited marked limitations in reliability performance, with survival probabilities falling significantly below the required threshold. The introduction of adaptive preventive thresholds in (ΔT, M_k) enhanced risk sensitivity by initiating interventions more aggressively near critical conditions, thereby reducing corrective failures. However, this improvement in reliability was achieved at the expense of higher preventive workload, without fundamentally altering the cost–reliability balance. The fully adaptive strategy (ΔT_k, M_k) demonstrated the most consistent alignment between inspection frequency, preventive aggressiveness, and system risk. By intensifying monitoring during high-risk phases and recalibrating intervention thresholds in real time, it significantly reduced the likelihood of catastrophic failures. Although it increased variability in inspection and intervention scheduling, it offered superior performance under the penalty-augmented criterion J_λ, highlighting the decisive role of adaptivity in reconciling cost efficiency with stringent reliability requirements.

From an engineering perspective, these findings underscore that the selection of an appropriate maintenance policy should be informed by the operational context and organizational priorities. In cost-sensitive environments where procedural simplicity and predictability are valued, static policies may remain acceptable despite their lower reliability. Conversely, in reliability-critical applications (such as aerospace, energy, or advanced manufacturing) adaptive strategies, particularly those that incorporate dynamic inspection intervals, provide substantial advantages by reducing exposure to undetected failures. The framework further illustrates that maintenance policies should not be judged solely on economic performance; compliance with reliability and risk constraints is paramount, as strategies that fail to respect these requirements are operationally infeasible regardless of apparent cost savings.

The study also opens several avenues for future research. Methodologically, the modeling framework could be enriched by incorporating alternative stochastic degradation processes, such as gamma or Lévy models, to capture wear phenomena not adequately represented by the Wiener process. The extension to multi-component systems and system-level dependencies is of particular importance, as interactions between components may significantly alter optimal maintenance strategies. From an optimization standpoint, the adaptive parameters governing inspection intervals and preventive thresholds could be systematically tuned using metaheuristic optimization or reinforcement learning, thereby enabling data-driven adaptation rules tailored to specific industrial contexts. Empirical validation constitutes another critical perspective: applying the framework to industrial case studies supported by degradation monitoring data and maintenance records would provide practical calibration and strengthen external validity. Furthermore, the integration of economic, environmental, and safety indicators within a unified decision-making framework would align maintenance optimization with broader objectives of sustainability and resilience, increasingly emphasized in contemporary asset management.

The near-equivalence of results across strategies is not a weakness but a meaningful diagnostic outcome: it identifies the threshold beyond which adaptive mechanisms must be intensified or redesigned to produce measurable benefits. This insight enriches current understanding of CBM policy design and validates the proposed simulation framework as a tool for uncovering such boundaries.

The absence of direct comparison with P–F or predictive maintenance policies reflects the study's methodological emphasis on internal consistency rather than cross-framework benchmarking. However, the developed architecture is readily extendable to incorporate these advanced strategies, providing a clear pathway for future comparative analyses that will contextualize adaptive CBM within the broader maintenance optimization landscape.

Beyond its methodological contributions, this study provides practical recommendations for engineering application. Adaptive parameters should be tuned within moderate ranges (α_T = 0.6–0.8, α_L = 0.4–0.6) to balance responsiveness and stability. When monitoring noise is significant, filtered degradation estimates and tightened preventive thresholds are recommended. Finally, hybrid adaptive–risk-constrained frameworks represent a promising direction for future implementation, ensuring that adaptivity enhances reliability without disproportionate cost growth.

ACKNOWLEDGMENT

We gratefully acknowledge the invaluable support and guidance provided by the Department of Mechanical Engineering, Energetic team, Mechanical and Industrial Systems (EMISys), Mohammadia School of Engineers, Mohammed V University, Rabat, Morocco. We also extend our appreciation to the anonymous reviewers for their insightful feedback.

REFERENCES

[1] Kalbfleisch, J.D., Prentice, R.L. (2002). The Statistical Analysis of Failure Time Data. John Wiley & Sons. https://doi.org/10.1002/9781118032985

[2] Wang, W.B. (2008). Condition-based maintenance modelling. In Complex System Maintenance Handbook, pp. 111-131. https://doi.org/10.1007/978-1-84800-011-

7_5
[3] Kharoufeh, J.P. (2003). Explicit results for wear processes in a Markovian environment. Operations Research Letters, 31(3): 237-244. https://doi.org/10.1016/S0167-6377(02)00229-8
[4] Deloux, E., Castanier, B., Bérenguer, C. (2009). Predictive maintenance policy for a gradually deteriorating system subject to stress. Reliability Engineering & System Safety, 94(2): 418-431. https://doi.org/10.1016/j.ress.2008.04.002
[5] Zhao, X.J., Fouladirad, M., Bérenguer, C., Bordes, L. (2010). Condition-based inspection/replacement policies for non-monotone deteriorating systems with environmental covariates. Reliability Engineering & System Safety, 95(8): 921-934. https://doi.org/10.1016/j.ress.2010.04.005
[6] Mustafa, M.A.S. (2025). Predictive reliability-driven optimization of spare parts management in aircraft fleets Using AI, IoT, and digital twin technologies. Journal of Engineering Management and Systems Engineering, 4(3): 218-236. https://doi.org/10.56578/jemse040305
[7] Cheikh, K., Boudi, E.M., Mokhliss, H., Rabi, R. (2024). Development and optimization of maintenance using the Monte Carlo method. International Journal of Industrial Engineering & Production Research, 35(3): 44-62. https://doi.org/10.22068/ijiepr.35.3.1994
[8] Wang, W. (2007). A prognosis model for wear prediction based on oil-based monitoring. Journal of the Operational Research Society, 58: 887-893. https://doi.org/10.1057/palgrave.jors.2602185
[9] Cheikh, K., Boudi, E.M., Rabi, R., Mokhliss, H., Ennaji, H. (2025). Evaluating the performance and robustness of PIR and QIR maintenance strategies using Monte Carlo method. Monte Carlo Methods and Applications, 31(1): 43-58. https://doi.org/10.1515/mcma-2025-2001
[10] Daya, A.A., Lazakis, I. (2024). Systems reliability and data-driven analysis for marine machinery maintenance planning and decision making. Machines, 12(5): 294. https://doi.org/10.3390/machines12050294
[11] Zio, E., Peloni, G. (2011). Particle filtering prognostic estimation of the remaining useful life of nonlinear components. Reliability Engineering & System Safety, 96(3): 403-409. https://doi.org/10.1016/j.ress.2010.08.009
[12] Yang, Y., Klutke, G.A. (2000). Improved inspection schemes for deteriorating equipment. Probability in the Engineering and Informational Sciences, 14(4): 445-460. https://doi.org/10.1017/S0269964800144043
[13] Grall, A., Dieulle, L., Bérenguer, C., Roussignol, M. (2002). Continuous-time predictive-maintenance scheduling for a deteriorating system. IEEE Transactions on Reliability, 51(2): 141-150. https://doi.org/10.1109/TR.2002.1011518
[14] Barker, C.T., Newby, M.J. (2009). Optimal non-periodic inspection for a multivariate degradation model. Reliability Engineering & System Safety, 94(1): 33-43. https://doi.org/10.1016/j.ress.2007.03.015
[15] Ponchet, A., Fouladirad, M., Grall, A. (2010). Assessment of a maintenance model for a multi-deteriorating mode system. Reliability Engineering & System Safety, 95(11): 1244-1254. https://doi.org/10.1016/j.ress.2010.06.021
[16] Karaoğlu, U., Mbah, O., Zeeshan, Q. (2023). Applications of Machine Learning in Aircraft Maintenance. Journal of Engineering Management and Systems Engineering, 2(1), 76-95. https://doi.org/10.56578/jemse020105
[17] Wang, F.J., Zhai, Z., Zhao, Z.B., Di, Y., Chen, X.F. (2024). Physics-informed neural network for lithium-ion battery degradation stable modeling and prognosis. Nature Communications, 15: 4332. https://doi.org/10.1038/s41467-024-48779-z
[18] Bigerelle, M., Iost, A. (1999). Bootstrap analysis of FCGR, application to the Paris relationship and to lifetime prediction. International Journal of Fatigue, 21(4): 299-307. https://doi.org/10.1016/S0142-1123(98)00076-0
[19] Kozin, F., Bogdanoff, J.L. (1989). Probabilistic models of fatigue crack growth: Results and speculations. Nuclear Engineering and Design, 115(1): 143-171. https://doi.org/10.1016/0029-5493(89)90267-7
[20] Zhang, C., Wu, P., Mu, S., Dong, Y. (2024). Stress ratio influence on Paris parameter and fatigue driving force pertinent to material properties. International Journal of Fatigue, 185: 108368. https://doi.org/10.1016/j.ijfatigue.2024.108368
[21] Chen, Z., Li, T., Xue, X., Zhou, Y., Jing, S. (2021). Fatigue reliability analysis and optimization of vibrator baseplate based on fuzzy comprehensive evaluation method. Engineering Failure Analysis, 127: 105357. https://doi.org/10.1016/j.engfailanal.2021.105357
[22] Lin, Y.K., Yang, J.N. (1983). On statistical moments of fatigue crack propagation. Engineering Fracture Mechanics, 18(2): 243-256. https://doi.org/10.1016/0013-7944(83)90136-4
[23] Kozin, F., Bogdanoff, J.L. (1981). A critical analysis of some probabilistic models of fatigue crack growth. Engineering Fracture Mechanics, 14(1): 59-89. https://doi.org/10.1016/0013-7944(81)90019-9
[24] Yang, J.N., Manning, S.D. (1996). A simple second order approximation for stochastic crack growth analysis. Engineering Fracture Mechanics, 53(5): 677-686. https://doi.org/10.1016/0013-7944(95)00130-1
[25] Xing, J., Zhong, O.P., Hong, Y.J. (1997). A simple log-normal random process approach of the fatigue crack growth considering the distribution of initial crack size and loading condition. International Journal of Pressure Vessels and Piping, 74(1): 7-12. https://doi.org/10.1016/S0308-0161(97)00058-6
[26] Wu, W.F., Ni, C.C. (2003). A study of stochastic fatigue crack growth modeling through experimental data. Probabilistic Engineering Mechanics, 18(2): 107-118. https://doi.org/10.1016/S0266-8920(02)00053-X
[27] Wu, W.F., Ni, C.C. (2004). Probabilistic models of fatigue crack propagation and their experimental verification. Probabilistic Engineering Mechanics, 19(3): 247-257. https://doi.org/10.1016/j.probengmech.2004.02.008
[28] Özekici, S. (1995). Optimal maintenance policies in random environments. European Journal of Operational Research, 82(2): 283-294. https://doi.org/10.1016/0377-2217(94)00264-D
[29] Cox, D.R. (1972). Regression models and life-tables. Journal of the Royal Statistical Society: Series B, 34(2): 187-220. http://www.jstor.org/stable/2985181.
[30] Cheikh, K., Boudi, E.M., Rabi, R., Mokhliss, H. (2024). Balancing the maintenance strategies to making decisions using Monte Carlo method. MethodsX, 13:

102819. https://doi.org/10.1016/j.mex.2024.102819
[31] Cheikh, K., Boudi, E.M., Rabi, R., Mokhliss, H. (2025). Influence of the system downtime cost rate on the performance and robustness of Periodic Inspection and Replacement and Quantitative Inspection and Replacement maintenance strategies using Monte Carlo method. Journal of Nondestructive Evaluation, Diagnostics and Prognostics of Engineering Systems, 8(1): 011005. https://doi.org/10.1115/1.4066115
[32] Cheikh, K., Boudi, E.M., Rabi, R., Mokhliss, H. (2025). A Monte Carlo method to decision-making in maintenance strategies. Journal of Nondestructive Evaluation, Diagnostics and Prognostics of Engineering Systems, 8(2): 021001. https://doi.org/10.1115/1.4066194
[33] Tijms, H.C. (2003). A First Course in Stochastic Models. John Wiley & Sons. https://doi.org/10.1002/047001363X
[34] Huynh, K.T., Barros, A., Bérenguer, C. (2012). Adaptive condition-based maintenance decision framework for deteriorating systems operating under variable environment and uncertain condition monitoring. Proceedings of the Institution of Mechanical Engineers, Part O: Journal of Risk and Reliability, 226(6): 602-623. https://doi.org/10.1177/1748006X12465718
[35] Karatzas, I., Shreve, S.E. (1998). Brownian Motion and Stochastic Calculus. Springer Science & Business Media. https://doi.org/10.1007/978-1-4612-0949-2
[36] Borodin, A.N., Salminen, P. (2002). Handbook of Brownian Motion - Facts and Formulae. Birkhäuser Basel. https://doi.org/10.1007/978-3-0348-8163-0
[37] Furubayashi, T., Nakano, T., Eckford, A., Yomo, T. (2015). Reliable end-to-end molecular communication with packet replication and retransmission. In 2015 IEEE Global Communications Conference (GLOBECOM), San Diego, CA, USA, pp. 1-6. https://doi.org/10.1109/GLOCOM.2015.7417465
[38] Kalman, R.E. (1960). A new approach to linear filtering and prediction problems. Journal of Fluids Engineering, 82(1): 35-45. https://doi.org/10.1115/1.3662552
[39] Protter, P.E. (2012). Stochastic differential equations. In Stochastic integration and differential equations, Berlin, pp. 249-361. https://doi.org/10.1007/978-3-662-10061-5_6
[40] Karatzas, I., Kou, S.G. (1998). Hedging American contingent claims with constrained portfolios. Finance and Stochastics, 2: 215-258. https://doi.org/10.1007/s007800050039
[41] Scarf, P.A. (2007). A framework for condition monitoring and condition-based maintenance. Quality Technology & Quantitative Management, 4(2): 301-312. https://doi.org/10.1080/16843703.2007.11673152
[42] Mobley, R.K. (2002). An Introduction to Predictive Maintenance. Elsevier. https://doi.org/10.1016/B978-0-7506-7531-4.X5000-3
[43] Al-Hussaini, E.K., Sultan, K.S. (2001). Ch. 5. Reliability and hazard based on finite mixture models. Handbook of Statistics, 20: 139-183. https://doi.org/10.1016/S0169-7161(01)20007-8
[44] Baldeaux, J., Platen, E. (2013). Functionals of Wiener processes. In Functionals of Multidimensional Diffusions with Applications to Finance, pp. 23-63. https://doi.org/10.1007/978-3-319-00747-2_2
[45] Li, R., Li, J., Song, Y., Wang, K., Luo, T., Lu, J. (2022). An optimal condition-based maintenance model for accelerated degrading products. In 12th International Conference on Quality, Reliability, Risk, Maintenance, and Safety Engineering (QR2MSE 2022), Emeishan, China, pp. 1838-1842. https://doi.org/10.1049/icp.2022.3136
[46] Law, A.M. (2007). Simulation Modeling and Analysis. McGraw-Hill, New York.
[47] Kaplan, E.L., Meier, P. (1958). Nonparametric estimation from incomplete observations. Journal of the American Statistical Association, 53(282): 457-481. https://doi.org/10.2307/2281868
[48] Shapiro, A., Dentcheva, D., Ruszczyński, A. (2021). MOS-SIAM Series on Optimization Lectures on Stochastic Programming: Modeling and Theory, Third Edition. SIAM. https://doi.org/10.1137/1.9781611976595
[49] Ross, S.M. (1995). Stochastic Processes. John Wiley & Sons.
[50] Jardine, A.K.S., Lin, D., Banjevic, D. (2006). A review on machinery diagnostics and prognostics implementing condition-based maintenance. Mechanical Systems and Signal Processing, 20(7): 1483-1510. https://doi.org/10.1016/j.ymssp.2005.09.012
[51] Simon, D. (2006). Optimal State Estimation: Kalman, H Infinity, and Nonlinear Approaches. Wiley-Interscience.
[52] Daher, A. (2018). Default diagnosis and prognosis for preventive and predictive maintenance. Application to a distillation column. Ph.D. Thesis, Normandie Université. https://tel.archives-ouvertes.fr/tel-01992688.

NOMENCLATURE

α_L	Adaptation coefficient for preventive threshold
α_T	Adaptation coefficient for inspection interval
β	Maximum admissible short-horizon failure probability
CBM	Condition-Based Maintenance
C_{avg}	Average long-run cost rate component in J_λ
C_{CM}	Cost of one corrective maintenance action
C_{insp}	Cost of one inspection
C_{PM}	Cost of one preventive maintenance action
CM	Corrective Maintenance
D_{avg}	Total downtime per run
δL_{safety}	Safety margin between preventive and failure thresholds
Δt	Numerical integration step (Euler–Maruyama discretization)
ΔT	Inspection interval (fixed or adaptive)
ΔT_{fix}	Fixed inspection interval
ΔT_k	Adaptive inspection interval at inspection k
ΔT_{max},ΔT_{min}	Maximum and minimum admissible inspection intervals
ε	Measurement noise (Gaussian random error)
I_{avg}	Inspections per run
J_λ	Penalty-augmented objective function
J_{lambda}	J_λ, penalty-augmented objective
KM	Kaplan–Meier reliability estimator
L_f	Failure threshold (critical degradation limit)
L_m	Fixed preventive maintenance threshold
$L_{m,k}$	Adaptive preventive maintenance threshold

	at inspection k
L_{min}	Lower admissible bound for adaptive preventive threshold
λ_{hit}	Penalty weight for short-horizon risk violation
λ_R	Penalty weight for reliability shortfall
MC	Monte Carlo simulation
μ	Drift coefficient of the Wiener degradation process
N_{CM}, N_{PM}	Number of corrective and preventive maintenance actions
N_{sim}	Number of Monte Carlo simulation replications
$Penalty_{hit}$	$\lambda_{hit} \cdot Pr$, λ_{hit}=1000
$Penalty_R$	$\lambda_{R} \cdot shortfall$, λ_R=10000
p_{hit}	Probability of failure between consecutive inspections
$\Phi(\cdot)$	Standard normal cumulative distribution function
PM	Preventive Maintenance
PM/CM	Ratio of preventive to corrective maintenance actions
PdM	Predictive Maintenance
$Pr[p_{hit}>\beta]$	Fraction of p_{Hit} of beta with β=0.05
R	Reliability by Kaplan–Meier survival at R_{time}
R_{min}	Minimum required reliability level
R_{min} - R	Reliability gap with R_{min}=0.95
R_{time}	Reliability at reporting horizon
R_{Rtime}	Survival at R_{time}=2000
RSE	Relative Standard Error
RUL	Residual Useful Life
$1[R \geq R_{min}]$	Meets required reliability
$\rho_{PM/CM}$	Ratio of PM to CM counts
σ	Diffusion coefficient (stochastic variability)
σ_{meas}	Standard deviation of measurement noise
s_C	Standard deviation of cost rate
s_{master}	Master random number generator seed
t_{CM}	Downtime due to corrective maintenance
t_{insp}	Downtime associated with each inspection
t_{PM}	Downtime due to preventive maintenance
T_{op}	Total operational horizon of the simulation
Var[C]	Variance of cost
W(t)	Standard Wiener process (Brownian motion)
X(t)	True degradation level at time t
$\hat{X}(t)$	Estimated degradation state at time t